A quasi-3D theory for functionally graded porous microbeams based on the modified strain gradient theory

Armagan Karamanli[a,*], Thuc P. Vo[b]

[a]Faculty of Engineering and Natural Sciences, Mechatronics Engineering, Bahcesehir University, Istanbul, Turkey.

[b]School of Engineering and Mathematical Sciences, La Trobe University, Bundoora, VIC 3086, Australia

[*]Corresponding author. E-mail: armaganfatih.karamanli@eng.bau.edu.tr (A. Karamanli)

Abstract

In this paper, the size-dependent responses of functionally graded (FG) porous microbeams using a quasi-3D theory and the modified strain gradient theory are investigated. Three different porosity distribution models of the FG porous microbeams are considered. By using the rule of mixture, all material properties including the material length scale parameters (MLSPs) are functions of the thickness, porosity coefficient and gradient index. The size-dependent governing equations are derived, and beam element is used to solve the problems. The verification of the proposed model is carried out and the effects of variable MLSP, porosity coefficient, gradient index and boundary conditions on the structural responses of FG porous microbeams are investigated. It can be observed that the effect of variable MLSP is significant and should be included for an accuracy analysis of the FG porous microbeams.

Keywords: variable MLSP; porosity coefficient; bending; vibration; buckling

1. Introduction

Due to the severe requirements from the industries such as military, nuclear, biomedical, electronics etc., the researchers have been devoting great effort to find not only the most effective solution but also the best approach to create the mathematical model of the engineering problems. Most effective solutions mainly depend on the advancement in the material technology. For instance, with the application of functionally graded materials (FGMs) which allow to control mechanical properties through the required directions, some of the deficiencies of the laminated composites in terms of high stress concentrations due to interlaminar discontinuities, passivity against high temperature working conditions etc. have been eliminated so far. Moreover, in many micro/nano electro-mechanical systems (MEMS/NEMS), the FGMs have been used due to their superior features which are available without any sacrifices in providing high stiffness to weight ratio and no interlaminar stress concentration and allowing to have lightweight structure design [1-8].

The structures used for the manufacturing of the MEMS/NEMS are mainly the beams, plates and shell. Unfortunately, the small size effect does not allow to investigate the mechanical behavior of these structures using the mathematical models based on the Classical Continuum Theories (CCTs). As a result, the researchers have been developing the Higher-order Continuum Theories (HCTs) accompanied with a material length scale parameter (MLSP) [9-11] to understand the nature of the mechanical analysis of the small size structures. The HCTs have been used by many researchers to study the mechanical behaviour of the MEMS/NEMS equipped with beams/plates/shells [12-27]. The review study dedicated to analysis of the microstructures based on the HCTs can be found in [28].

The modified couple stress theory (MCST) developed by Yang et al. [27], which includes only one MLSP, can be classified as the most popular HCTs due to having the couple stress tensor as symmetric. Though the implementation of MCST can be found easier than other HCTs, it is incapable of capturing the size effect due to missing the dilatation and deviatoric stretch gradient tensors in its formulation [29]. Therefore, the modified strain gradient theory (MSGT [11]) considered these tensors in its formulation by including three MLSPs. The size dependent mechanical behaviours of isotropic structures have been investigated successfully by employing the MSGT [30-39]. Moreover, the MSGT was also applied for the structural responses of the FG microbeams [40-45], microplates [45-51] and microshells [52]. The vibration behaviour of the FG microbeams were presented by Ansari et al. [40] based on the First-order beam theory (FBT). The comparisons between the results obtained by three models (CCT, MCST and MSGT) was carried out by Ansari and his colleagues [41] to investigate the mechanical responses of FG Timoshenko microbeams. Sahmani et al. [42] applied the MSGT for the nonlinear frequency analysis of FG microbeams by employing differential quadrature method (DQM). A trigonometric shear deformable beam theory was used by Akgoz and Civalek [43] for buckling analysis and Lei et al. [44] for bending and vibration analysis of the FG microbeams. Analytical solutions were obtained for the free vibrations of the FG microplates based on the Navier method and a higher-order shear deformable plate theory [45]. Various shear deformable plate theories were employed for the mechanical analysis of the FG microplates by using DQM [46, 47]. Isogeometric analysis (IGA) was employed to investigate linear [48] and nonlinear [49] flexural analysis of the FG microplates. The structural analysis of the FG sandwich microplates was studied by employing the IGA and MSGT [50, 51]. Zhang et al. [52] studied the free vibration responses of FG strain gradient cylindrical microshells.

The above studies focus only on the FG perfect structures based on the MSGT. However, one can notice that the production of the mechanical parts used in the MEMS/NEMS is not carried out in perfect operating conditions including the inadequate quality practices, inexperienced labors, lack of maintenance procedures, etc. Accordingly, the imperfection in the FG structures mainly called as microporosities can be found. With the increasing the microporosity volume fraction, the structural responses of the FG micro/nano structures could be affected profoundly [53-61]. On the other hand, to provide a lightweight design, the microporosity volume fraction can be used as a tool to tailor the material properties in the desired directions. As a result, the investigations based on the mechanical analysis of FG strain gradient porous microbeams are important and necessary. As far as authors are aware, the studies related to this topic are very limited in the open literature. By using Navier method, Wang et al. [62] studied the bending and free vibration behaviors of FG strain gradient microbeams. Arani et al. [63] presented the vibration responses of the FG imperfect sandwich microbeams having two flexoelectric layers on the top and bottom based on the strain gradient Euler-Bernoulli beam theory and Navier method. The structural analysis mentioned above were carried out based on the constant MLSP which can be considered as a material property [64-65]. Since the MLSP is an elastic property, it can be also affected with the variation of the material properties through the elastic body and porosity distribution. The studies related to variable MLSP are very limited. The MSGT was implemented for the flexural and free vibration analysis of Euler-Bernoulli microbeams based on the variable MLSP approach [66]. Different shear deformations theories were employed to investigate the bending, buckling and free vibration responses of the FG microbeams based on the MCST with a variable MLSP [67-69]. As far as the authors are aware there is no study for the structural analysis of FG porous strain gradient microbeams based on a quasi-3D theory for various boundary conditions. In this study, by using a quasi-3D theory and the MSGT, the size dependent responses of the FG porous microbeams are investigated. Three different porosity distribution models of the FG porous microbeams are considered. By using the rule of mixture, all material properties including the MLSPs are functions of the thickness, porosity coefficient and gradient index. The equations of motion are constructed by employing the Lagrange's equations. The verification of the present model is performed, and then parametric studies are carried out to investigate the effects of small size, variable MLSP, porosity distribution, gradient index, and boundary conditions on the responses of FG porous microbeams.

2. Governing Equations Based on the Strain Gradient FE Model

2.1 FG Porous Microbeams

In Fig. 1, a FG microbeam with three porosity distribution models is presented with its geometrical properties (L-Length, h-height and b-width). The effective material properties $P(z)$ including Young's modulus E(z), Poisson's ratio $\nu(z)$, mass density $\rho(z)$ and MLSP $\ell(z)$ can be defined as:

$$P(z) = P_c\left(V_c(z) - \frac{\alpha_0(z)}{2}\right) + P_m\left(V_m(z) - \frac{\alpha_0(z)}{2}\right) \tag{1}$$

where $P_{c,m}$ is material property and $V_{c,m}$ is volume fraction of ceramic and metal, α_0 is the porosity coefficient.

It should be noted that in Eq.(1), $V_c(z) = \left(\frac{1}{2} + \frac{z}{h}\right)^{p_z}$ and $V_c(z) + V_m(z) = 1$ where p_z is gradient index

The effective material properties of the FG porous microbeams can be obtained by the rule of mixture [70]:

FGM I

$$E(z) = (E_c - E_m)\left(\frac{1}{2} + \frac{z}{h}\right)^{p_z} + E_m - \frac{\alpha_0}{2}(E_c + E_m) \tag{2a}$$

$$\nu(z) = (\nu_c - \nu_m)\left(\frac{1}{2} + \frac{z}{h}\right)^{p_z} + \nu_m - \frac{\alpha_0}{2}(\nu_c + \nu_m) \tag{2b}$$

$$\rho(z) = (\rho_c - \rho_m)\left(\frac{1}{2} + \frac{z}{h}\right)^{p_z} + \rho_m - \frac{\alpha_0}{2}(\rho_c + \rho_m) \tag{2c}$$

$$\ell(z) = (\ell_c - \ell_m)\left(\frac{1}{2} + \frac{z}{h}\right)^{p_z} + \ell_m - \frac{\alpha_0}{2}(\ell_c + \ell_m) \tag{2d}$$

FGM II

$$E(z) = (E_c - E_m)\left(\frac{1}{2} + \frac{z}{h}\right)^{p_z} + E_m - \frac{\alpha_0}{2}\left(1 - \frac{2|z|}{h}\right)(E_c + E_m) \tag{3a}$$

$$\nu(z) = (\nu_c - \nu_m)\left(\frac{1}{2} + \frac{z}{h}\right)^{p_z} + \nu_m - \frac{\alpha_0}{2}\left(1 - \frac{2|z|}{h}\right)(\nu_c + \nu_m) \tag{3b}$$

$$\rho(z) = (\rho_c - \rho_m)\left(\frac{1}{2} + \frac{z}{h}\right)^{p_z} + \rho_m - \frac{\alpha_0}{2}\left(1 - \frac{2|z|}{h}\right)(\rho_c + \rho_m) \tag{3c}$$

$$\ell(z) = (\ell_c - \ell_m)\left(\frac{1}{2} + \frac{z}{h}\right)^{p_z} + \ell_m - \frac{\alpha_0}{2}\left(1 - \frac{2|z|}{h}\right)(\ell_c + \ell_m) \quad (3d)$$

FGM III

$$E(z) = (E_c - E_m)\left(\frac{1}{2} + \frac{z}{h}\right)^{p_z} + E_m - \log\left(1 + \frac{\alpha_0}{2}\right)\left(1 - \cos\left(\frac{\pi z}{h}\right)\right)(E_c + E_m) \quad (4a)$$

$$\nu(z) = (\nu_c - \nu_m)\left(\frac{1}{2} + \frac{z}{h}\right)^{p_z} + \nu_m - \log\left(1 + \frac{\alpha_0}{2}\right)\left(1 - \cos\left(\frac{\pi z}{h}\right)\right)(\nu_m + \nu_c) \quad (4b)$$

$$\rho(z) = (\rho_c - \rho_m)\left(\frac{1}{2} + \frac{z}{h}\right)^{p_z} + \rho_m - \log\left(1 + \frac{\alpha_0}{2}\right)\left(1 - \cos\left(\frac{\pi z}{h}\right)\right)(\rho_c + \rho_m) \quad (4c)$$

$$\ell(z) = (\ell_c - \ell_m)\left(\frac{1}{2} + \frac{z}{h}\right)^{p_z} + \ell_m - \log\left(1 + \frac{\alpha_0}{2}\right)\left(1 - \cos\left(\frac{\pi z}{h}\right)\right)(\ell_c + \ell_m) \quad (4d)$$

2.2 Formulation of the MSGT

For a linear elastic microbeam, the strain energy ($\mathcal{U}$) can be presented in the form of:

$$\mathcal{U} = \frac{1}{2}\int_V \left(\sigma_{ij}\varepsilon_{ij} + m_{ij}\chi_{ij} + p_i\gamma_i + \tau_{ijk}\eta_{ijk}\right)d\,\mathcal{V}, \quad i,j,k = 1,2,3 \quad (5)$$

where σ_{ij} and ε_{ij} are the stress and strain tensors, the higher order stress tensors can be given as m_{ij}, p_i and τ_{ijk} and associated strain tensors χ_{ij}, γ_i and η_{ijk} are the symmetric curvature, the dilatation and deviatoric stretch gradient tensors, respectively.

The strain tensors based on the displacement field (u_1, u_2, u_3) can be presented as follows:

$$\varepsilon_{ij} = \frac{1}{2}\left(\frac{\partial u_i}{\partial x_j} + \frac{\partial u_j}{\partial x_i}\right) \quad (6a)$$

$$\chi_{ij} = \frac{1}{4}\left(e_{imn}\frac{\partial^2 u_n}{\partial x_{mj}^2} + e_{jmn}\frac{\partial^2 u_n}{\partial x_{mi}^2}\right) \quad (6b)$$

$$\gamma_i = \frac{\partial \varepsilon_{mm}}{\partial x_i} \quad (6c)$$

$$\eta_{ijk} = \frac{1}{3}\left(\frac{\partial \varepsilon_{jk}}{\partial x_i} + \frac{\partial \varepsilon_{ki}}{\partial x_j} + \frac{\partial \varepsilon_{ij}}{\partial x_k}\right) - \frac{1}{15}\left[\delta_{ij}\left(\frac{\partial \varepsilon_{mm}}{\partial x_k} + 2\frac{\partial \varepsilon_{mk}}{\partial x_m}\right) + \delta_{jk}\left(\frac{\partial \varepsilon_{mm}}{\partial x_i} + 2\frac{\partial \varepsilon_{mi}}{\partial x_m}\right) + \delta_{ki}\left(\frac{\partial \varepsilon_{mm}}{\partial x_j} + 2\frac{\partial \varepsilon_{mj}}{\partial x_m}\right)\right] \quad (6d)$$

The linear elastic constitutive relations can be given in the form of:

$$\sigma_{ij} = \left(\frac{E(z)}{1+\nu(z)}\right)\varepsilon_{ij} + \left[\frac{\nu(z)E(z)}{(1+\nu(z))(1-2\nu(z))}\right]\varepsilon_{kk}\delta_{ij} \quad (7a)$$

$$p_i = \left(\frac{E(z){\ell_0}^2(z)}{1+\nu(z)}\right)\gamma_i \quad (7b)$$

$$\tau_{ijk} = \left(\frac{E(z){\ell_1}^2(z)}{1+\nu(z)}\right)\eta_{ijk} \quad (7c)$$

$$m_{ij} = \left(\frac{E(z){\ell_2}^2(z)}{1+\nu(z)}\right)\chi_{ij} \quad (7d)$$

where ℓ_0, ℓ_1 and ℓ_2 are three MLSPs related to the dilatation, deviatoric stretch gradient and symmetric curvature.

2.3 Variational Formulation Based on a Quasi-3D Theory

The displacement fields of the FG porous microbeams are based on a quasi-3D theory [60, 61] as:

$$u_1(x,z,t) = U(x,z,t) = u(x,t) - f_1(z)\frac{\partial w_b(x,t)}{\partial x} + f_2(z)\frac{\partial w_s(x,t)}{\partial x} \quad (8a)$$

$$u_3(x,t) = W(x,t) = w_b(x,t) + w_s(x,t) + f_3(z)\, w_z(x,t) \quad (8b)$$

$$f_1(z) = \frac{4z^3}{3h^2}, f_2(z) = z - \frac{8z^3}{3h^2} \ \ and \ \ f_3(z) = 1 - \frac{4z^2}{h^2} \quad (8c)$$

where u is the in-plane displacement, w_b, w_s *and* w_z are the bending, shear and thickness stretching components of the vertical displacement, respectively.

The nonzero strains can be obtained:

$$\varepsilon_x = \frac{\partial U}{\partial x} = u' - f_1 w_b'' + f_2 w_s'' \quad (9a)$$

$$\varepsilon_z = \frac{\partial W}{\partial z} = {f_3}' w_z \quad (9b)$$

$$\varepsilon_{xz} = \frac{\gamma_{xz}}{2} = \frac{\partial W}{\partial x} + \frac{\partial U}{\partial z} = \frac{1}{2} f_3 (w_b' + 2w_s' + w_z') \qquad (9c)$$

The strain tensor associated with the higher order stresses can be given by using Eq. (6):

$$\chi_{xy} = \frac{1}{4} [-(1 + f_1{}')w_b'' - (1 - f_2{}')w_s'' - f_3 w_z''] \qquad (10a)$$

$$\chi_{yz} = \frac{1}{2}\left(\frac{\partial \theta_z}{\partial y} + \frac{\partial \theta_y}{\partial z}\right) = \frac{1}{4} (-f_1{}'' w_b' + f_2{}'' w_s' - f_3{}' w_z') \qquad (10b)$$

$$\gamma_x = u'' - f_1 w_b''' + f_2 w_s''' + f_3{}' w_z' \qquad (10c)$$

$$\gamma_z = -f_1{}' w_b'' + f_2{}' w_s'' + f_3{}'' w_z \qquad (10d)$$

$$\eta_{xxx} = \frac{1}{5} [2u'' - 2f_1 w_b''' - f_3{}' w_b' + 2f_2 w_s''' - 2f_3{}' w_s' - f_3{}' w_z'] \qquad (10e)$$

$$\eta_{zzz} = \frac{1}{5} [f_1{}' w_b'' - f_3 w_b'' - f_2{}' w_s'' - 2f_3 w_s'' + 2f_3{}'' w_z - f_3 w_z''] \qquad (10f)$$

$$\eta_{yyx} = \eta_{yxy} = \eta_{xyy} = \frac{1}{15} [-3u'' + 3f_1 w_b''' - f_3{}' w_b' - 3f_2 w_s''' - 2f_3{}' w_s' - 2f_3{}' w_z'] \qquad (10g)$$

$$\eta_{zzx} = \eta_{zxz} = \eta_{xzz} = \frac{1}{15} [-3u'' + 3f_1 w_b''' + 4f_3{}' w_b' - 3f_2 w_s''' + 8f_3{}' w_s' + 8f_3{}' w_z'] \qquad (10h)$$

$$\eta_{xxz} = \eta_{xzx} = \eta_{zxx} = \frac{1}{15} [-4f_1{}' w_b'' + 4f_3 w_b'' + 8f_3 w_s'' + 4f_2{}' w_s'' + 4f_3 w_z'' - 3f_3{}'' w_z] \qquad (10i)$$

$$\eta_{yyz} = \eta_{yzy} = \eta_{zyy} = \frac{1}{15} [f_1{}' w_b'' - f_3 w_b'' - f_2{}' w_s'' - 2f_3 w_s'' - 3f_3{}'' w_z - f_3 w_z''] \qquad (10j)$$

$$\chi_{xx} = \chi_{yy} = \chi_{zz} = \chi_{xz} = \gamma_y = \eta_{zzy} = \eta_{zyz} = \eta_{yzz} = \eta_{yyy} = \eta_{xyz} = \eta_{yzx} = \eta_{zxy} = \eta_{xzy} = \eta_{zyx} = \eta_{yxz} = 0 \qquad (10k)$$

The relations of stresses and strains can be given by:

$$\begin{Bmatrix} \sigma_x \\ \sigma_z \\ \sigma_{xz} \end{Bmatrix} = \begin{bmatrix} Q_{11} & Q_{13} & 0 \\ Q_{13} & Q_{33} & 0 \\ 0 & 0 & Q_{44} \end{bmatrix} \begin{Bmatrix} \varepsilon_x \\ \varepsilon_z \\ 2\varepsilon_{xz} \end{Bmatrix} \qquad (11a)$$

$$Q_{11}(z) = Q_{33}(z) = \frac{E(z)(1 - v(z))}{(1 - 2v(z))(1 + v(z))} \qquad (11b)$$

$$Q_{13}(z) = \frac{E(z)v(z)}{(1 - 2v(z))(1 + v(z))} \qquad (11c)$$

$$Q_{44}(z) = \frac{E(z)}{2(1 + v(z))} \qquad (11d)$$

$$\begin{Bmatrix} p_x \\ p_z \end{Bmatrix} = \frac{E(z){\ell_0}^2(z)}{1 + \nu(z)} \begin{Bmatrix} \gamma_x \\ \gamma_z \end{Bmatrix} \qquad (11e)$$

$$\begin{Bmatrix} \tau_{xxx} \\ \tau_{zzz} \\ \tau_{xyy} \\ \tau_{xzz} \\ \tau_{zxx} \\ \tau_{zyy} \end{Bmatrix} = \frac{E(z){\ell_1}^2(z)}{1 + \nu(z)} \begin{Bmatrix} \eta_{xxx} \\ \eta_{zzz} \\ \eta_{xyy} \\ \eta_{xzz} \\ \eta_{zxx} \\ \eta_{zyy} \end{Bmatrix} \qquad (11f)$$

$$\begin{Bmatrix} m_{xy} \\ m_{yz} \end{Bmatrix} = \frac{E(z){\ell_2}^2(z)}{1 + \nu(z)} \begin{Bmatrix} \chi_{xy} \\ \chi_{yz} \end{Bmatrix} \qquad (11g)$$

The strain energy ($\mathcal{U}$) of the system can be obtained:

$$\mathcal{U} = \frac{1}{2}\int_V (\sigma_x\varepsilon_x + \sigma_z\varepsilon_z + \sigma_{xz}\gamma_{xz} + p_x\gamma_x + p_z\gamma_z + \tau_{xxx}\eta_{xxx} + \tau_{zzz}\eta_{zzz} + 3\tau_{xyy}\eta_{xyy} + 3\tau_{xzz}\eta_{xzz} + 3\tau_{zxx}\eta_{zxx} + 3\tau_{zyy}\eta_{zyy} + 2m_{xy}\chi_{xy} + 2m_{yz}\chi_{yz})dV \qquad (12)$$

By substituting Eq. (11) into Eq. (12), the following expression of $\mathcal{U}$ can be derived:

$$\mathcal{U} = \frac{1}{2}\int_V \left[(Q_{11}{\varepsilon_x}^2 + 2Q_{13}\varepsilon_x\varepsilon_z + Q_{11}{\varepsilon_z}^2 + Q_{44}{\gamma_{xz}}^2) + \frac{E{\ell_0}^2}{1+\nu}({\gamma_x}^2 + {\gamma_z}^2) + \frac{E{\ell_1}^2}{1+\nu}({\eta_{xxx}}^2 + {\eta_{zzz}}^2 + 3{\eta_{xyy}}^2 + 3{\eta_{xzz}}^2 + 3{\eta_{zxx}}^2 + 3{\eta_{zyy}}^2) + \frac{E{\ell_2}^2}{1+\nu}\left(2{\chi_{xy}}^2 + 2{\chi_{yz}}^2\right)\right] dV \tag{13}$$

where

$${\varepsilon_x}^2 = \left(\frac{\partial u}{\partial x}\right)^2 + {f_1}^2\left(\frac{\partial^2 w_b}{\partial x^2}\right)^2 + {f_2}^2\left(\frac{\partial^2 w_s}{\partial x^2}\right)^2 - 2f_1\left(\frac{\partial u}{\partial x}\right)\left(\frac{\partial^2 w_b}{\partial x^2}\right) + 2f_2\left(\frac{\partial u}{\partial x}\right)\left(\frac{\partial^2 w_s}{\partial x^2}\right) - 2f_1 f_2\left(\frac{\partial^2 w_b}{\partial x^2}\right)\left(\frac{\partial^2 w_s}{\partial x^2}\right) \tag{14a}$$

$$\varepsilon_x\varepsilon_z = f_3{}'\left(\frac{\partial u}{\partial x}\right)w_z - f_3{}' f_1\left(\frac{\partial^2 w_b}{\partial x^2}\right)w_z + f_3{}' f_2\left(\frac{\partial^2 w_s}{\partial x^2}\right)w_z \tag{14b}$$

$${\varepsilon_z}^2 = (f_3{}')^2 {w_z}^2 \tag{14c}$$

$${\gamma_{xz}}^2 = (f_3)^2\left[\left(\frac{\partial w_b}{\partial x}\right)^2 + 4\left(\frac{\partial w_s}{\partial x}\right)^2 + \left(\frac{\partial w_z}{\partial x}\right)^2 + 4\left(\frac{\partial w_b}{\partial x}\right)\left(\frac{\partial w_s}{\partial x}\right) + 2\left(\frac{\partial w_b}{\partial x}\right)\left(\frac{\partial w_z}{\partial x}\right) + 4\left(\frac{\partial w_s}{\partial x}\right)\left(\frac{\partial w_z}{\partial x}\right)\right] \tag{14d}$$

$${\chi_{xy}}^2 = \frac{1}{16}\left[\left(1 + \frac{df_1}{dz}\right)^2\left(\frac{d^2 w_b}{dx^2}\right)^2 + \left(1 - \frac{df_2}{dz}\right)^2\left(\frac{d^2 w_s}{dx^2}\right)^2 + {f_3}^2\left(\frac{d^2 w_z}{dx^2}\right)^2 + 2\left(1 + \frac{df_1}{dz}\right)\left(1 - \frac{df_2}{dz}\right)\left(\frac{d^2 w_b}{dx^2}\right)\left(\frac{d^2 w_s}{dx^2}\right) + 2\left(1 + \frac{df_1}{dz}\right)f_3\left(\frac{d^2 w_b}{dx^2}\right)\left(\frac{d^2 w_z}{dx^2}\right) + 2\left(1 - \frac{df_2}{dz}\right)f_3\left(\frac{d^2 w_s}{dx^2}\right)\left(\frac{d^2 w_z}{dx^2}\right)\right] \tag{14e}$$

$$\chi_{yz}{}^2 = \frac{1}{16}\left[\left(\frac{d^2f_1}{dz^2}\right)^2\left(\frac{dw_b}{dx}\right)^2 + \left(\frac{d^2f_2}{dz^2}\right)^2\left(\frac{dw_s}{dx}\right)^2 + \left(\frac{df_3}{dz}\right)^2\left(\frac{dw_z}{dx}\right)^2 - 2\left(\frac{d^2f_1}{dz^2}\right)\left(\frac{d^2f_2}{dz^2}\right)\left(\frac{dw_b}{dx}\right)\left(\frac{dw_s}{dx}\right) + 2\left(\frac{d^2f_1}{dz^2}\right)\left(\frac{df_3}{dz}\right)\left(\frac{dw_b}{dx}\right)\left(\frac{dw_z}{dx}\right) - 2\left(\frac{d^2f_2}{dz^2}\right)\left(\frac{df_3}{dz}\right)\left(\frac{dw_s}{dx}\right)\left(\frac{dw_z}{dx}\right)\right] \quad (14f)$$

$$\gamma_x{}^2 = \left(\frac{d^2u}{dx^2}\right)^2 + f_1{}^2\left(\frac{d^3w_b}{dx^3}\right)^2 + f_2{}^2\left(\frac{d^3w_s}{dx^3}\right)^2 + \left(\frac{df_3}{dz}\right)^2\left(\frac{dw_z}{dx}\right)^2 - 2f_1\left(\frac{d^2u}{dx^2}\right)\left(\frac{d^3w_b}{dx^3}\right) + 2f_2\left(\frac{d^2u}{dx^2}\right)\left(\frac{d^3w_s}{dx^3}\right) + 2\left(\frac{df_3}{dz}\right)\left(\frac{d^2u}{dx^2}\right)\left(\frac{dw_z}{dx}\right) - 2f_1f_2\left(\frac{d^3w_b}{dx^3}\right)\left(\frac{d^3w_s}{dx^3}\right) - 2f_1\left(\frac{df_3}{dz}\right)\left(\frac{d^3w_b}{dx^3}\right)\left(\frac{dw_z}{dx}\right) + 2f_2\left(\frac{df_3}{dz}\right)\left(\frac{d^3w_s}{dx^3}\right)\left(\frac{dw_z}{dx}\right) \quad (14g)$$

$$\gamma_z{}^2 = \left(\frac{df_1}{dz}\right)^2\left(\frac{d^2w_b}{dx^2}\right)^2 + \left(\frac{df_2}{dz}\right)^2\left(\frac{d^2w_s}{dx^2}\right)^2 + \left(\frac{d^2f_3}{dz^2}\right)^2 w_z{}^2 - 2\left(\frac{df_1}{dz}\right)\left(\frac{df_2}{dz}\right)\left(\frac{d^2w_b}{dx^2}\right)\left(\frac{d^2w_s}{dx^2}\right) - 2\left(\frac{df_1}{dz}\right)\left(\frac{d^2f_3}{dz^2}\right)\left(\frac{d^2w_b}{dx^2}\right)w_z + 2\left(\frac{df_2}{dz}\right)\left(\frac{d^2f_3}{dz^2}\right)\left(\frac{d^2w_s}{dx^2}\right)w_z \quad (14h)$$

$$\eta_{xxx}{}^2 = \frac{1}{25}\left[4\left(\frac{d^2u}{dx^2}\right)^2 - 8f_1\left(\frac{d^2u}{dx^2}\right)\left(\frac{d^3w_b}{dx^3}\right) - 4\left(\frac{df_3}{dz}\right)\left(\frac{d^2u}{dx^2}\right)\left(\frac{dw_b}{dx}\right) + 8f_2\left(\frac{d^2u}{dx^2}\right)\left(\frac{d^3w_s}{dx^3}\right) - 8\left(\frac{df_3}{dz}\right)\left(\frac{d^2u}{dx^2}\right)\left(\frac{dw_s}{dx}\right) - 8\left(\frac{df_3}{dz}\right)\left(\frac{d^2u}{dx^2}\right)\left(\frac{dw_z}{dx}\right) + 4f_1{}^2\left(\frac{d^3w_b}{dx^3}\right)^2 + \left(\frac{df_3}{dz}\right)^2\left(\frac{dw_b}{dx}\right)^2 + 4f_1\left(\frac{df_3}{dz}\right)\left(\frac{d^3w_b}{dx^3}\right)\left(\frac{dw_b}{dx}\right) - 8f_1f_2\left(\frac{d^3w_b}{dx^3}\right)\left(\frac{d^3w_s}{dx^3}\right) + 8f_1\left(\frac{df_3}{dz}\right)\left(\frac{d^3w_b}{dx^3}\right)\left(\frac{dw_s}{dx}\right) - 4f_2\left(\frac{df_3}{dz}\right)\left(\frac{dw_b}{dx}\right)\left(\frac{d^3w_s}{dx^3}\right) + 4\left(\frac{df_3}{dz}\right)^2\left(\frac{dw_b}{dx}\right)\left(\frac{dw_s}{dx}\right) + 4\left(\frac{df_3}{dz}\right)^2\left(\frac{dw_b}{dx}\right)\left(\frac{dw_z}{dx}\right) + 8f_1\left(\frac{df_3}{dz}\right)\left(\frac{d^3w_b}{dx^3}\right)\left(\frac{dw_z}{dx}\right) + 4f_2{}^2\left(\frac{d^3w_s}{dx^3}\right)^2 + 4\left(\frac{df_3}{dz}\right)^2\left(\frac{dw_s}{dx}\right)^2 - 8f_2\left(\frac{df_3}{dz}\right)\left(\frac{d^3w_s}{dx^3}\right)\left(\frac{dw_s}{dx}\right) - 8f_2\left(\frac{df_3}{dz}\right)\left(\frac{d^3w_s}{dx^3}\right)\left(\frac{dw_z}{dx}\right) + 8\left(\frac{df_3}{dz}\right)^2\left(\frac{dw_s}{dx}\right)\left(\frac{dw_z}{dx}\right) + 4\left(\frac{df_3}{dz}\right)^2\left(\frac{dw_z}{dx}\right)^2\right] \quad (14i)$$

$$\eta_{zzz}{}^2 = \frac{1}{25}\Bigg[\left(\frac{df_1}{dz}\right)^2\left(\frac{d^2w_b}{dx^2}\right)^2 - 2\left(\frac{df_1}{dz}\right)f_3\left(\frac{d^2w_b}{dx^2}\right)^2 + (f_3)^2\left(\frac{d^2w_b}{dx^2}\right)^2$$

$$- 2\left(\frac{df_1}{dz}\right)\left(\frac{df_2}{dz}\right)\left(\frac{d^2w_b}{dx^2}\right)\left(\frac{d^2w_s}{dx^2}\right) - 4\left(\frac{df_1}{dz}\right)(f_3)\left(\frac{d^2w_b}{dx^2}\right)\left(\frac{d^2w_s}{dx^2}\right)$$

$$+ 2\left(\frac{df_2}{dz}\right)(f_3)\left(\frac{d^2w_b}{dx^2}\right)\left(\frac{d^2w_s}{dx^2}\right) + 4(f_3)^2\left(\frac{d^2w_b}{dx^2}\right)\left(\frac{d^2w_s}{dx^2}\right)$$

$$- 2\left(\frac{df_1}{dz}\right)(f_3)\left(\frac{d^2w_b}{dx^2}\right)\left(\frac{d^2w_z}{dx^2}\right) + 2(f_3)^2\left(\frac{d^2w_b}{dx^2}\right)\left(\frac{d^2w_z}{dx^2}\right)$$

$$+ 4\left(\frac{df_1}{dz}\right)\left(\frac{d^2f_3}{dz^2}\right)\left(\frac{d^2w_b}{dx^2}\right)w_z - 4(f_3)\left(\frac{d^2f_3}{dz^2}\right)\left(\frac{d^2w_b}{dx^2}\right)w_z + \left(\frac{df_2}{dz}\right)^2\left(\frac{d^2w_s}{dx^2}\right)^2$$

$$+ 4\left(\frac{df_2}{dz}\right)(f_3)\left(\frac{d^2w_s}{dx^2}\right)^2 + 4(f_3)^2\left(\frac{d^2w_s}{dx^2}\right)^2 + 2\left(\frac{df_2}{dz}\right)(f_3)\left(\frac{d^2w_s}{dx^2}\right)\left(\frac{d^2w_z}{dx^2}\right)$$

$$+ 4(f_3)^2\left(\frac{d^2w_s}{dx^2}\right)\left(\frac{d^2w_z}{dx^2}\right) - 4\left(\frac{df_2}{dz}\right)\left(\frac{d^2f_3}{dz^2}\right)\left(\frac{d^2w_s}{dx^2}\right)w_z$$

$$- 8(f_3)\left(\frac{d^2f_3}{dz^2}\right)\left(\frac{d^2w_s}{dx^2}\right)w_z + (f_3)^2\left(\frac{d^2w_z}{dx^2}\right)^2$$

$$+ 4\left(\frac{d^2f_3}{dz^2}\right)^2 w_z{}^2 - 4(f_3)\left(\frac{d^2f_3}{dz^2}\right)w_z\left(\frac{d^2w_z}{dx^2}\right)\Bigg] \qquad (14j)$$

$$3{\eta_{xyy}}^2 = \frac{3}{225}\left[9\left(\frac{d^2u}{dx^2}\right)^2 + 6\left(\frac{df_3}{dz}\right)\left(\frac{d^2u}{dx^2}\right)\left(\frac{dw_b}{dx}\right) - 18f_1\left(\frac{d^2u}{dx^2}\right)\left(\frac{d^3w_b}{dx^3}\right)\right.$$
$$+ 12\left(\frac{df_3}{dz}\right)\left(\frac{d^2u}{dx^2}\right)\left(\frac{dw_s}{dx}\right) + 18f_2\left(\frac{d^2u}{dx^2}\right)\left(\frac{d^3w_s}{dx^3}\right) + 12\left(\frac{df_3}{dz}\right)\left(\frac{d^2u}{dx^2}\right)\left(\frac{dw_z}{dx}\right)$$
$$+ 9{f_1}^2\left(\frac{d^3w_b}{dx^3}\right)^2 - 6f_1\left(\frac{df_3}{dz}\right)\left(\frac{d^3w_b}{dx^3}\right)\left(\frac{dw_b}{dx}\right) + \left(\frac{df_3}{dz}\right)^2\left(\frac{dw_b}{dx}\right)^2$$
$$- 18f_1f_2\left(\frac{d^3w_b}{dx^3}\right)\left(\frac{d^3w_s}{dx^3}\right) - 12f_1\left(\frac{df_3}{dz}\right)\left(\frac{d^3w_b}{dx^3}\right)\left(\frac{dw_s}{dx}\right)$$
$$+ 6f_2\left(\frac{df_3}{dz}\right)\left(\frac{dw_b}{dx}\right)\left(\frac{d^3w_s}{dx^3}\right) + 4\left(\frac{df_3}{dz}\right)^2\left(\frac{dw_b}{dx}\right)\left(\frac{dw_s}{dx}\right)$$
$$- 12f_1\left(\frac{df_3}{dz}\right)\left(\frac{d^3w_b}{dx^3}\right)\left(\frac{dw_z}{dx}\right) + 4\left(\frac{df_3}{dz}\right)^2\left(\frac{dw_b}{dx}\right)\left(\frac{dw_z}{dx}\right) + 9{f_2}^2\left(\frac{d^3w_s}{dx^3}\right)^2$$
$$+ 4\left(\frac{df_3}{dz}\right)^2\left(\frac{dw_s}{dx}\right)^2 + 12f_2\left(\frac{df_3}{dz}\right)\left(\frac{d^3w_s}{dx^3}\right)\left(\frac{dw_s}{dx}\right)$$
$$\left.+ 12f_2\left(\frac{df_3}{dz}\right)\left(\frac{d^3w_s}{dx^3}\right)\left(\frac{dw_z}{dx}\right) + 8\left(\frac{df_3}{dz}\right)^2\left(\frac{dw_s}{dx}\right)\left(\frac{dw_z}{dx}\right) + 4\left(\frac{df_3}{dz}\right)^2\left(\frac{dw_z}{dx}\right)^2\right] \quad (14k)$$

$$
\begin{aligned}
3{\eta_{xzz}}^2 = \frac{3}{225}\Bigg[& 9\left(\frac{d^2u}{dx^2}\right)^2 - 18f_1\left(\frac{d^2u}{dx^2}\right)\left(\frac{d^3w_b}{dx^3}\right) - 24\left(\frac{df_3}{dz}\right)\left(\frac{d^2u}{dx^2}\right)\left(\frac{dw_b}{dx}\right) \\
& + 18f_2\left(\frac{d^2u}{dx^2}\right)\left(\frac{d^3w_s}{dx^3}\right) - 48\left(\frac{df_3}{dz}\right)\left(\frac{d^2u}{dx^2}\right)\left(\frac{dw_s}{dx}\right) - 48\left(\frac{df_3}{dz}\right)\left(\frac{d^2u}{dx^2}\right)\left(\frac{dw_z}{dx}\right) \\
& + 9{f_1}^2\left(\frac{d^3w_b}{dx^3}\right)^2 + 24f_1\left(\frac{df_3}{dz}\right)\left(\frac{d^3w_b}{dx^3}\right)\left(\frac{dw_b}{dx}\right) + 16\left(\frac{df_3}{dz}\right)^2\left(\frac{dw_b}{dx}\right)^2 \\
& - 18f_1f_2\left(\frac{d^3w_b}{dx^3}\right)\left(\frac{d^3w_s}{dx^3}\right) + 48f_1\left(\frac{df_3}{dz}\right)\left(\frac{d^3w_b}{dx^3}\right)\left(\frac{dw_s}{dx}\right) \\
& - 24f_2\left(\frac{df_3}{dz}\right)\left(\frac{dw_b}{dx}\right)\left(\frac{d^3w_s}{dx^3}\right) + 64\left(\frac{df_3}{dz}\right)^2\left(\frac{dw_b}{dx}\right)\left(\frac{dw_s}{dx}\right) \\
& + 48f_1\left(\frac{df_3}{dz}\right)\left(\frac{d^3w_b}{dx^3}\right)\left(\frac{dw_z}{dx}\right) + 64\left(\frac{df_3}{dz}\right)^2\left(\frac{dw_b}{dx}\right)\left(\frac{dw_z}{dx}\right) + 9{f_2}^2\left(\frac{d^3w_s}{dx^3}\right)^2 \\
& - 48f_2\left(\frac{df_3}{dz}\right)\left(\frac{d^3w_s}{dx^3}\right)\left(\frac{dw_s}{dx}\right) + 64\left(\frac{df_3}{dz}\right)^2\left(\frac{dw_s}{dx}\right)^2 \\
& - 48f_2\left(\frac{df_3}{dz}\right)\left(\frac{d^3w_s}{dx^3}\right)\left(\frac{dw_z}{dx}\right) + 128\left(\frac{df_3}{dz}\right)^2\left(\frac{dw_s}{dx}\right)\left(\frac{dw_z}{dx}\right) \\
& + 64\left(\frac{df_3}{dz}\right)^2\left(\frac{dw_z}{dx}\right)^2\Bigg] \qquad (14l)
\end{aligned}
$$

$$3\eta_{zxx}{}^2 = \frac{3}{225}\Bigg[16(f_3)^2\left(\frac{d^2w_b}{dx^2}\right)^2 - 32\left(\frac{df_1}{dz}\right)(f_3)\left(\frac{d^2w_b}{dx^2}\right)^2 + 16\left(\frac{df_1}{dz}\right)^2\left(\frac{d^2w_b}{dx^2}\right)^2$$

$$+ 64(f_3)^2\left(\frac{d^2w_b}{dx^2}\right)\left(\frac{d^2w_s}{dx^2}\right) - 64\left(\frac{df_1}{dz}\right)(f_3)\left(\frac{d^2w_b}{dx^2}\right)\left(\frac{d^2w_s}{dx^2}\right)$$

$$+ 32\left(\frac{df_2}{dz}\right)(f_3)\left(\frac{d^2w_b}{dx^2}\right)\left(\frac{d^2w_s}{dx^2}\right) - 32\left(\frac{df_1}{dz}\right)\left(\frac{df_2}{dz}\right)\left(\frac{d^2w_b}{dx^2}\right)\left(\frac{d^2w_s}{dx^2}\right)$$

$$+ 32(f_3)^2\left(\frac{d^2w_b}{dx^2}\right)\left(\frac{d^2w_z}{dx^2}\right) - 32\left(\frac{df_1}{dz}\right)(f_3)\left(\frac{d^2w_b}{dx^2}\right)\left(\frac{d^2w_z}{dx^2}\right)$$

$$- 24(f_3)\left(\frac{d^2f_3}{dz^2}\right)\left(\frac{d^2w_b}{dx^2}\right)w_z + 24\left(\frac{df_1}{dz}\right)\left(\frac{d^2f_3}{dz^2}\right)\left(\frac{d^2w_b}{dx^2}\right)w_z + 64(f_3)^2\left(\frac{d^2w_s}{dx^2}\right)^2$$

$$+ 64\left(\frac{df_2}{dz}\right)f_3\left(\frac{d^2w_s}{dx^2}\right)^2 + 16\left(\frac{df_2}{dz}\right)^2\left(\frac{d^2w_s}{dx^2}\right)^2 + 64(f_3)^2\left(\frac{d^2w_s}{dx^2}\right)\left(\frac{d^2w_z}{dx^2}\right)$$

$$+ 32\left(\frac{df_2}{dz}\right)(f_3)\left(\frac{d^2w_s}{dx^2}\right)\left(\frac{d^2w_z}{dx^2}\right) - 48(f_3)\left(\frac{d^2f_3}{dz^2}\right)\left(\frac{d^2w_s}{dx^2}\right)w_z$$

$$- 24\left(\frac{df_2}{dz}\right)\left(\frac{d^2f_3}{dz^2}\right)\left(\frac{d^2w_s}{dx^2}\right)w_z$$

$$+ 16(f_3)^2\left(\frac{d^2w_z}{dx^2}\right)^2 + 9\left(\frac{d^2f_3}{dz^2}\right)^2 w_z{}^2 - 24(f_3)\left(\frac{d^2f_3}{dz^2}\right)\left(\frac{d^2w_z}{dx^2}\right)w_z\Bigg] \qquad (14m)$$

$$
\begin{aligned}
3\eta_{zyy}{}^2 = \frac{3}{225}\Bigg[& (f_3)^2\left(\frac{d^2w_b}{dx^2}\right)^2 - 2\left(\frac{df_1}{dz}\right) f_3\left(\frac{d^2w_b}{dx^2}\right)^2 + \left(\frac{df_1}{dz}\right)^2\left(\frac{d^2w_b}{dx^2}\right)^2 \\
& + 4\,(f_3)^2\left(\frac{d^2w_b}{dx^2}\right)\left(\frac{d^2w_s}{dx^2}\right) - 4\left(\frac{df_1}{dz}\right) f_3\left(\frac{d^2w_b}{dx^2}\right)\left(\frac{d^2w_s}{dx^2}\right) \\
& + 2\left(\frac{df_2}{dz}\right) f_3\left(\frac{d^2w_b}{dx^2}\right)\left(\frac{d^2w_s}{dx^2}\right) - 2\left(\frac{df_1}{dz}\right)\left(\frac{df_2}{dz}\right)\left(\frac{d^2w_b}{dx^2}\right)\left(\frac{d^2w_s}{dx^2}\right) \\
& + 2\,(f_3)^2\left(\frac{d^2w_b}{dx^2}\right)\left(\frac{d^2w_z}{dx^2}\right) - 2\left(\frac{df_1}{dz}\right) f_3\left(\frac{d^2w_b}{dx^2}\right)\left(\frac{d^2w_z}{dx^2}\right) \\
& + 6f_3\left(\frac{d^2f_3}{dz^2}\right)\left(\frac{d^2w_b}{dx^2}\right)w_z - 6\left(\frac{df_1}{dz}\right)\left(\frac{d^2f_3}{dz^2}\right)\left(\frac{d^2w_b}{dx^2}\right)w_z + 4(f_3)^2\left(\frac{d^2w_s}{dx^2}\right)^2 \\
& + 4\left(\frac{df_2}{dz}\right) f_3\left(\frac{d^2w_s}{dx^2}\right)^2 + \left(\frac{df_2}{dz}\right)^2\left(\frac{d^2w_s}{dx^2}\right)^2 + 4(f_3)^2\left(\frac{d^2w_s}{dx^2}\right)\left(\frac{d^2w_z}{dx^2}\right) \\
& + 2\left(\frac{df_2}{dz}\right) f_3\left(\frac{d^2w_s}{dx^2}\right)\left(\frac{d^2w_z}{dx^2}\right) + 12f_3\left(\frac{d^2f_3}{dz^2}\right)\left(\frac{d^2w_s}{dx^2}\right)w_z \\
& + 6\left(\frac{df_2}{dz}\right)\left(\frac{d^2f_3}{dz^2}\right)\left(\frac{d^2w_s}{dx^2}\right)w_z + (f_3)^2\left(\frac{d^2w_z}{dx^2}\right)^2 \\
& + 9\left(\frac{d^2f_3}{dz^2}\right)^2 w_z{}^2 + 6f_3\left(\frac{d^2f_3}{dz^2}\right)\left(\frac{d^2w_z}{dx^2}\right)w_z\Bigg] \qquad (14n)
\end{aligned}
$$

The potential energy (V) and kinetic energy (K) of the systems are derived in the form of:

$$
V = -\frac{1}{2}\int_0^L N_0\left\{\left(\frac{\partial w_b}{\partial x}\right)^2 + 2\frac{\partial w_b}{\partial x}\frac{\partial w_s}{\partial x} + \left(\frac{\partial w_s}{\partial x}\right)^2\right\}dx - \int_0^L q(w_b + w_s + f_3(z)w_z)dx \qquad (15a)
$$

$$
\begin{aligned}
K = \frac{1}{2}\int_0^L \Bigg[& I_0\left\{\left(\frac{\partial u}{\partial t}\right)^2 + \left(\frac{\partial w_b}{\partial t}\right)^2 + \left(\frac{\partial w_s}{\partial t}\right)^2 + 2\left(\frac{\partial w_b}{\partial t}\right)\left(\frac{\partial w_s}{\partial t}\right)\right\} - 2I_1\frac{\partial u}{\partial t}\frac{\partial^2 w_b}{\partial x\partial t} + I_2\left(\frac{\partial^2 w_b}{\partial x\partial t}\right)^2 \\
& + 2J_1\frac{\partial u}{\partial t}\frac{\partial^2 w_s}{\partial x\partial t} + 2J_2\left\{\left(\frac{\partial w_b}{\partial t}\right)\left(\frac{\partial w_z}{\partial t}\right) + \left(\frac{\partial w_s}{\partial t}\right)\left(\frac{\partial w_z}{\partial t}\right)\right\} - 2J_3\frac{\partial^2 w_b}{\partial x\partial t}\frac{\partial^2 w_s}{\partial x\partial t} \\
& + K_1\left(\frac{\partial^2 w_s}{\partial x\partial t}\right)^2 + K_2\left(\frac{\partial w_z}{\partial t}\right)^2\Bigg]dx \qquad (15b)
\end{aligned}
$$

where N_0 and q(x) are the axial and uniform load, t is the time, and inertial coefficients are given by

$$(I_0, I_1, I_2, J_1, J_2, J_3, K_1, K_2) = \int_{-\frac{h}{2}}^{+\frac{h}{2}} \rho \left(1, f_1, {f_1}^2, f_2, f_3, f_1 f_2, {f_2}^2, {f_3}^2\right) dz \quad (16)$$

The total energy (Π) of the systems can be obtained from Eqs. (13)-(15) in the following form:

$$\Pi = U + V - K \quad (17)$$

2.4 FE Strain Gradient Model

FE strain gradient model is developed here to obtain the numerical solutions for the structural analysis of the FG porous microbeams. The displacement functions $u(x,t)$, $w_b(x,t)$, $w_s(x,t)$ and $w_z(x,t)$ can be expressed with Hermite-cubic polynomial function based on the total energy in Eq. (17) given above as:

$$u(x,t) = \sum_{j=1}^{4} u_j \varphi_j(x) e^{i\omega t}, \quad (18a)$$

$$w_b(x,t) = \sum_{j=1}^{4} {w_b}_j \varphi_j(x) e^{i\omega t}, \quad (18b)$$

$$w_s(x,t) = \sum_{j=1}^{4} {w_s}_j \varphi_j(x) e^{i\omega t}, \quad (18c)$$

$$w_z(x,t) = \sum_{j=1}^{4} {w_z}_j \varphi_j(x) e^{i\omega t}, \quad (18d)$$

where ω is the natural frequency.

The unknowns per node can be given by:

$$u_j = [u, u_{,x}] \quad (19a)$$

$${w_b}_j = [w_b, w_{b,x}] \quad (19b)$$

$${w_s}_j = [w_s, w_{s,x}] \quad (19c)$$

$${w_z}_j = [w_z, w_{z,x}] \quad (19d)$$

By using the Lagrange's equations, equations of motion of the FG porous microbeams can be obtained:

$$\frac{\partial \Pi}{\partial q_j} - \frac{\partial}{\partial t}\left(\frac{\partial \Pi}{\partial \dot{q}_j}\right) = 0 \tag{20}$$

where q_j representing the values of $(u_j, w_{b\,j}, w_{s\,j}, w_{z\,j})$.

The structural responses of FG porous microbeams can be solved via the stiffness matrix $[K_{kl}]$, mass matrix $[M_{kl}]$ and geometric stiffness matrix $[G_{kl}]$ and F_k is the nodal force vector as below:

$$\begin{bmatrix} [K_{11}] & [K_{12}] & [K_{13}] & [K_{14}] \\ [K_{12}]^T & [K_{22}] & [K_{23}] & [K_{24}] \\ [K_{13}]^T & [K_{23}]^T & [K_{33}] & [K_{34}] \\ [K_{14}]^T & [K_{24}]^T & [K_{34}]^T & [K_{44}] \end{bmatrix} \begin{Bmatrix} \{u_j\} \\ \{w_{b\,j}\} \\ \{w_{s\,j}\} \\ \{w_{z\,j}\} \end{Bmatrix} = \begin{Bmatrix} \{0\} \\ \{F_2\} \\ \{F_3\} \\ \{F_4\} \end{Bmatrix} \tag{21a}$$

$$\left(\begin{bmatrix} [K_{11}] & [K_{12}] & [K_{13}] & [K_{14}] \\ [K_{12}]^T & [K_{22}] & [K_{23}] & [K_{24}] \\ [K_{13}]^T & [K_{23}]^T & [K_{33}] & [K_{34}] \\ [K_{14}]^T & [K_{24}]^T & [K_{34}]^T & [K_{44}] \end{bmatrix} - N_0 \begin{bmatrix} [0] & [0] & [0] & [0] \\ [0]^T & [G_{22}] & [G_{23}] & [0] \\ [0]^T & [G_{23}]^T & [G_{33}] & [0] \\ [0]^T & [0]^T & [0]^T & [0] \end{bmatrix} \right) \begin{Bmatrix} \{u_j\} \\ \{w_{b\,j}\} \\ \{w_{s\,j}\} \\ \{w_{z\,j}\} \end{Bmatrix} = \begin{Bmatrix} \{0\} \\ \{0\} \\ \{0\} \\ \{0\} \end{Bmatrix} \tag{21b}$$

$$\left(\begin{bmatrix} [K_{11}] & [K_{12}] & [K_{13}] & [K_{14}] \\ [K_{12}]^T & [K_{22}] & [K_{23}] & [K_{24}] \\ [K_{13}]^T & [K_{23}]^T & [K_{33}] & [K_{34}] \\ [K_{14}]^T & [K_{24}]^T & [K_{34}]^T & [K_{44}] \end{bmatrix} - \omega^2 \begin{bmatrix} [M_{11}] & [M_{12}] & [M_{13}] & [0] \\ [M_{12}]^T & [M_{22}] & [M_{23}] & [M_{24}] \\ [M_{13}]^T & [M_{23}]^T & [M_{33}] & [M_{34}] \\ [M_{14}]^T & [M_{24}]^T & [M_{34}]^T & [M_{44}] \end{bmatrix} \right) \begin{Bmatrix} \{u_j\} \\ \{w_{b\,j}\} \\ \{w_{s\,j}\} \\ \{w_{z\,j}\} \end{Bmatrix} = \begin{Bmatrix} \{0\} \\ \{0\} \\ \{0\} \\ \{0\} \end{Bmatrix} \tag{21c}$$

Their components are presented in the form of:

$$K_{11}(i,j) = \int_0^l A\, \varphi_{i,x}\varphi_{j,x}dx + \int_0^l \left[A_\gamma + \frac{2}{5}A_\eta\right]\varphi_{i,xx}\varphi_{j,xx}dx \tag{22a}$$

$$K_{12}(i,j) = -\int_0^l B\, \varphi_{i,x}\varphi_{j,xx}dx - \int_0^l \left[B_\gamma + \frac{2}{5}B_\eta\right]\varphi_{i,xx}\varphi_{j,xxx}dx - \frac{1}{5}\int_0^l Y_\eta\, \varphi_{i,xx}\varphi_{j,x}dx \tag{22b}$$

$$K_{13}(i,j) = \int_0^l B_s\,\varphi_{i,x}\varphi_{j,xx}dx + \int_0^l \left[C_\gamma + \frac{2}{5}C_\eta\right]\varphi_{i,xx}\varphi_{j,xxx}dx - \frac{2}{5}\int_0^l Y_\eta\,\varphi_{i,xx}\varphi_{j,x}dx \qquad (22c)$$

$$K_{14}(i,j) = \int_0^l X\,\varphi_{i,x}\varphi_j dx + \int_0^l \left[D_\gamma - \frac{2}{5}Y_\eta\right]\varphi_{i,xx}\varphi_{j,x}dx \qquad (22d)$$

$$K_{22}(i,j) = \int_0^l \left[D + \frac{1}{8}A_\chi + H_\gamma + \frac{4}{15}Z_\eta + \frac{4}{15}S_\eta - \frac{8}{15}X_\eta\right]\varphi_{i,xx}\varphi_{j,xx}dx$$
$$+ \int_0^l \left[A_s + \frac{1}{8}P_\chi + \frac{4}{15}R_\eta\right]\varphi_{i,x}\varphi_{j,x}dx + \int_0^l \left[F_\gamma + \frac{2}{5}D_\eta\right]\varphi_{i,xxx}\varphi_{j,xxx}dx + \int_0^l \frac{2}{5}F_{s\eta}\,\varphi_{i,xxx}\varphi_{j,x}dx \qquad (22e)$$

$$K_{23}(i,j) = \int_0^l \left[-D_s + \frac{1}{8}B_\chi - Y_\gamma - \frac{4}{15}B_{s\eta} + \frac{4}{15}C_{s\eta} + \frac{8}{15}S_\eta - \frac{8}{15}X_\eta\right]\varphi_{i,xx}\varphi_{j,xx}dx$$
$$+ \int_0^l \left[2A_s - \frac{1}{8}R_\chi + \frac{8}{15}R_\eta\right]\varphi_{i,x}\varphi_{j,x}dx - \int_0^l \left[X_\gamma + \frac{2}{5}H_\eta\right]\varphi_{i,xxx}\varphi_{j,xxx}dx + \int_0^l \frac{2}{5}F_{s\eta}\,\varphi_{i,xxx}\varphi_{j,x}dx$$
$$- \int_0^l \frac{1}{5}H_{s\eta}\,\varphi_{i,x}\varphi_{j,xxx}dx \qquad (22f)$$

$$K_{24}(i,j) = \int_0^l \left[-Y - P_\gamma + \frac{1}{5}Y_{s\eta} - \frac{1}{5}D_{s\eta}\right]\varphi_{i,xx}\varphi_j dx + \int_0^l \left[A_s + \frac{1}{8}S_\chi + \frac{8}{15}R_\eta\right]\varphi_{i,x}\varphi_{j,x}dx$$

$$+ \int_0^l \left[\frac{1}{8}D_\chi - \frac{4}{15}X_\eta + \frac{4}{15}S_\eta\right]\varphi_{i,xx}\varphi_{i,xx}dx + \int_0^l \left[-Z_\gamma + \frac{2}{5}F_{s\eta}\right]\varphi_{i,xxx}\varphi_{j,x}dx \qquad (22g)$$

$$K_{33}(i,j) = \int_0^l \left[H + \frac{1}{8}C_\chi + S_\gamma + \frac{4}{15}P_\eta + \frac{16}{15}C_{s\eta} + \frac{16}{15}S_\eta\right]\varphi_{i,xx}\varphi_{j,xx}dx - \frac{4}{5}\int_0^l H_{s\eta}\,\varphi_{i,xxx}\varphi_{j,x}dx$$

$$+\int_0^l \left[R_\gamma + \frac{2}{5}F_\eta\right]\varphi_{i,xxx}\varphi_{j,xxx}dx + \int_0^l \left[4A_s + \frac{1}{8}X_\chi + \frac{16}{15}R_\eta\right]\varphi_{i,x}\varphi_{j,x}dx \quad (22h)$$

$$K_{34}(i,j) = \int_0^l \left[Y_s + B_{s\gamma} - \frac{1}{5}R_{s\eta} - \frac{2}{5}D_{s\eta}\right]\varphi_{i,xx}\varphi_j dx + \int_0^l \left[2A_s - \frac{1}{8}Z_\chi + \frac{16}{15}R_\eta\right]\varphi_{i,x}\varphi_{j,x}dx$$

$$+\int_0^l \left[\frac{1}{8}H_\chi + \frac{4}{15}C_{s\eta} + \frac{8}{15}S_\eta\right]\varphi_{i,xx}\varphi_{j,xx}dx + \int_0^l \left[A_{s\gamma} - \frac{2}{5}H_{s\eta}\right]\varphi_{i,xxx}\varphi_{j,x}dx \quad (22i)$$

$$K_{44}(i,j) = \int_0^l \left[Z + D_{s\gamma} + \frac{2}{5}A_{s\eta}\right]\varphi_i\varphi_j dx + \int_0^l \left[A_s + \frac{1}{8}Y_\chi + C_{s\gamma} + \frac{16}{15}R_\eta\right]\varphi_{i,x}\varphi_{j,x}dx$$

$$+\int_0^l \left[\frac{1}{8}F_\chi + \frac{4}{15}S_\eta\right]\varphi_{i,xx}\varphi_{j,xx}dx - \frac{2}{5}\int_0^l D_{s\eta}\,\varphi_{i,xx}\varphi_j dx \quad (22j)$$

$$M_{11}(i,j) = \int_0^l I_0\,\varphi_i\varphi_j dx \quad (22k)$$

$$M_{12}(i,j) = -\int_0^l I_1\,\varphi_i\varphi_{j,x}dx \quad (22l)$$

$$M_{13}(i,j) = \int_0^l J_1\,\varphi_i\varphi_{j,x}dx \quad (22m)$$

$$M_{22}(i,j) = \int_0^l I_0\,\varphi_i\varphi_j dx + \int_0^l I_2\,\varphi_{i,x}\varphi_{j,x}dx \quad (22n)$$

$$M_{23}(i,j) = \int_0^l I_0\, \varphi_i \varphi_j dx - \int_0^l J_3\, \varphi_{i,x} \varphi_{j,x} dx \tag{22o}$$

$$M_{24}(i,j) = \int_0^l J_2\, \varphi_i \varphi_j dx \tag{22p}$$

$$M_{33}(i,j) = \int_0^l I_0\, \varphi_i \varphi_j dx + \int_0^l K_1\, \varphi_{i,x} \varphi_{j,x} dx \tag{22q}$$

$$M_{34}(i,j) = \int_0^l J_2\, \varphi_i \varphi_j dx \tag{22r}$$

$$M_{44}(i,j) = \int_0^l K_2\, \varphi_i \varphi_j dx \tag{22s}$$

$$G_{22}(i,j) = -N_0 \int_0^l \varphi_{i,x} \varphi_{j,x}\, dx \tag{22t}$$

$$G_{23}(i,j) = -N_0 \int_0^l \varphi_{i,x} \varphi_{j,x}\, dx \tag{22u}$$

$$G_{33}(i,j) = -N_0 \int_0^l \varphi_{i,x} \varphi_{j,x}\, dx \tag{22v}$$

$$F_2(i) = -\int_0^l q(x) \varphi_i\, dx \tag{22w}$$

$$F_3(i) = -\int_0^l q(x)\varphi_i \, dx \qquad (22x)$$

Here, the stiffness coefficients can be defined by:

$$(A, B, B_s, D, D_s, H, Z) = \int_{-h/2}^{+h/2} Q_{11} \left(1, f_1, f_2, {f_1}^2, f_1 f_2, {f_2}^2, {f_3{'}}^2\right) dz \qquad (22a)$$

$$A_s = \int_{-h/2}^{+h/2} Q_{44} {f_3}^2 dz \qquad (23b)$$

$$(X, Y, Y_s) = \int_{-h/2}^{+h/2} Q_{13} {f_3}'(1, f_1, f_2) dz \qquad (23c)$$

$$(A_\chi, B_\chi, C_\chi, D_\chi, F_\chi, H_\chi, X_\chi, Y_\chi, Z_\chi, P_\chi, R_\chi, S_\chi) = \int_{-h/2}^{+h/2} \frac{E{\ell_2}^2}{1+\nu} \Big[(1+{f_1}')^2, (1+{f_1}')(1-{f_2}'), (1-{f_2}')^2, (1+{f_1}')f_3, {f_3}^2, (1 - {f_2}')f_3, {f_2{''}}^2, {f_3{'}}^2, {f_2}''{f_3}', {f_1{''}}^2, {f_1}''{f_2}'', {f_1}''{f_3}'\Big] dz \qquad (23d)$$

$$(A_\gamma, B_\gamma, C_\gamma, D_\gamma, F_\gamma, H_\gamma, X_\gamma, Y_\gamma, Z_\gamma, P_\gamma, R_\gamma, S_\gamma, A_{s\gamma}, B_{s\gamma}, C_{s\gamma}, D_{s\gamma}) = \int_{-h/2}^{+h/2} \frac{E{\ell_0}^2}{1+\nu} \Big[1, f_1, f_2, {f_3}', {f_1}^2, {f_1{'}}^2, f_1 f_2, {f_1}'{f_2}', f_1{f_3}', {f_1}'{f_3}'', {f_2}^2, {f_2{'}}^2, f_2{f_3}', {f_2}'{f_3}'', {f_3{'}}^2, {f_3{''}}^2\Big] dz \qquad (23e)$$

$$(A_\eta, B_\eta, C_\eta, D_\eta, F_\eta, H_\eta, X_\eta, Y_\eta, Z_\eta, P_\eta, R_\eta, S_\eta, A_{s\eta}, B_{s\eta}, C_{s\eta}, D_{s\eta}, F_{s\eta}, H_{s\eta}, Y_{s\eta}, R_{s\eta}) = \int_{-\frac{h}{2}}^{+\frac{h}{2}} \frac{E{\ell_1}^2}{1+\nu} \Big[1, f_1, f_2, {f_1}^2, {f_2}^2, f_1 f_2, {f_1}'f_3, {f_3}', {f_1{'}}^2, {f_2{'}}^2, {f_3{'}}^2, {f_3}^2, {f_3{''}}^2, {f_1}'{f_2}', {f_2}'f_3, f_3{f_3}'', f_1{f_3}', f_2{f_3}', {f_1}'{f_3}'', {f_2}'{f_3}''\Big] dz \qquad (23f)$$

3. Numerical Examples

In this section, various examples of FG porous microbeams are analyzed to show the accuracy of the present theory and then investigate the effects of small size, porosity coefficients (α_0), variable MLSP (ℓ), gradient index (p_z), and boundary conditions (BCs) on their responses. These microbeams have material properties (Al: $E_m = 70\ GPa$, $\nu_m = 0.3$, $\rho_m = 2702\ kg/m^3$; SiC: $E_c = 427\ GPa$, $\nu_c = 0.17$, $\rho_c = 3100\ kg/m^3$. Three MLSPs are assumed to be the same value $\ell = \ell_0 = \ell_1 = \ell_2$ and varied via the thickness, porosity coefficients and gradient index, see Eqs. (2d) - (4d) for details. Two cases are considered in this section, constant MLSP ($\ell_c = \ell_m$) and variable MLSP ($\ell_c \neq \ell_m$). Unless mentioned otherwise, for constant MLSP, $\ell = \ell_m = 15\ \mu m$ and for variable MLSP ($\ell = \ell_m = 15\ \mu m$) for Al and ($\ell = \ell_c = 22.5\ \mu m$) for SiC [40, 67, 69]. The results are presented based on the dimensionless fundamental frequency (DFF) (λ), critical buckling load (DCBL) (N_{cr}) and mid-span deflection (DMD) ($\bar{w}$):

$$\lambda = \frac{\omega L^2}{h}\sqrt{\frac{\rho_m}{E_m}} \tag{24a}$$

$$N_{cr} = N_0 \frac{12L^2}{E_c h^3} \tag{24b}$$

$$\bar{w} = w\frac{10^3 E_m h^3}{qL^4} \tag{24c}$$

3.1 Verification studies

The verification is performed by comparing the numerical results of constant MLSP with those obtained from the MCST/MSGT using various theories such as the classical beam theory (CBT), First-order beam theory (FBT), sinusoidal beam theory (SBT) and third-order beam theory (TBT) as well as a quasi-3D based on TBT (Q3D TBT). Since there are no available results for FG porous microbeams using a Q3D and the MSGT, two cases of verification were considered: (1) FG microbeams using the FBT/SBT/TBT and MSGT; (2) FG porous microbeams using the FBT/Q3D and MCST.

Tables 1-5 contain the dimensionless deflections, frequencies and buckling loads of the FG microbeams $(L/h = 10)$. They are compared with those presented by Ansari et al. [40] (FBT), Lei et al. [44] (SBT) and Karamanli and Vo [73] (TBT) for three models (CCT, MCST and MSGT) in Tables 1 and 2. There is the slightly difference in three models between the present results and those from previous studies [40, 44, 73], which do not take into account normal strain effect. In order to take into account this effect, Trinh et al. [71] generated Navier solutions for the FG microbeams based on a Q3D TBT and MCST in Tables 3-5. The present results are in excellent agreement with those with and without Poisson's effect from previous paper [71]. As expected, size effect is more pronounced for very small beam $(h/\ell_m = 1)$ and for buckling responses than frequency and displacement ones.

In order to verify further, FGM I and II porous microbeams are considered and their frequencies and buckling loads are given in Tables 6 and 7. The reference MCST solutions were obtained with generalized differential quadrature method using the CBT/FBT [58, 59] and finite element model [72] using a Q3D TBT. Again, the current results show good agreement with previous ones, which demonstrates the validation of the present theory. Some new results from current model using the MCST/MSGT are also given in Tables 3-7. The inclusion of Poisson's effect and three MLSPs in the MSGT leads to increase frequencies and buckling loads and decrease displacements.

3.2 Parameter studies

The size-dependent responses of FG porous microbeams $(L/h = 5, 20)$ with various values of porosity coefficients (α_0), variable MLSP (ℓ), gradient index (p_z), and three BCs including C-C, S-S and C-F are studied.

The results of the FG microbeams are given in Tables 8-10. It can be observed that the results obtained from constant MLSP are significantly different from those from variable MLSP. As the MLSP of SiC ($\ell_c = 22.5\ \mu m$) is larger compared to that of Al ($\ell_m = 15\ \mu m$), the displacements become smaller and buckling loads and frequencies become bigger considerably. The ratios of results from variable MLSP to those from constant one of S-S FG microbeams is plotted in Fig. 2. These ratios reach unity as gradient index and dimensionless (h/ℓ_m) increase. It is interesting to observe that effect of variable MLSP is minimal for axial vibration but significant for flexural one (Table 8). For examples, these ratios are 1.01 for axial vibration and 1.25, 1.16, 1.06 for flexural vibration with ($p_z = 1$), respectively.

Three types of FG porous microbeams (FGM I, II and III) are analysed and their results are given in Tables 11-20. Among them, the DMDs of FGM III are the smallest and those of FGM I are the biggest. It should be noted that for porous microbeams, even ($\ell_c = \ell_m$), MLSP is also variable due to porosity coefficient ($\ell_c = \ell_m \neq \ell$). Therefore, three types of results ($\ell_c = \ell_m = \ell$) and ($\ell_c = \ell_m \neq \ell$) as well as ($\ell_c \neq \ell_m \neq \ell$) are compared to investigate the effect of the MLSP. Due to porosity coefficient ($\alpha_0 = 0.1$) in the MLSP, FG porous microbeam with ($\ell_c = \ell_m \neq \ell$) has lower buckling load and frequency but higher displacement compared to one without it ($\ell_c = \ell_m = \ell$). Fig. 3 also shows the ratios between the results of MSGT obtained from variable MLPS and constant one of S-S FG porous microbeams. Due to an increase in the stiffness, the ratios of DFFs and DCBLs are higher than unity and those of DMDs are lower than unity. The difference of the results by using two models (constant and variable MLSP) become negligible as h/ℓ_m increases. It confirms again that the variation of MLSP should be included in the analysis of FG microbeams.

The variation of results ratios, which are between those from the MSGT and MCST versus h/ℓ_m and α_0 of S-S microbeams and $p_z = 5$ are plotted in Figs. 4 and 5. Regardless of the value of porosity coefficient, these ratios have the same trend. Size effect is significant when beam's thickness is very small at micron scale ($h/\ell_m = 1$), these ratios are appoximately 2.25, 1.50 and 0.48. As (h/ℓ_m) increases, they finally approach unity as ($h/\ell_m = 20$). It means that the MSGT should be employed in the range of $h/\ell_m \in [1,20]$. From that point, the results of MSGT and MCST are slightly different. Besides, the porosity effect is more pronouced for the FG porous microbeams with lower values of (h/ℓ_m) (Fig. 4).

Figs. 6 and 7 illustrate the 3D variation results of the three porous FG microbeams with (h/ℓ_m), p_z, and α_0. It can be seen that that increasing α_0 leads to the decrease in the natural frequencies and buckling loads. The displacements increase when p_z , (h/ℓ_m) and α_0 increase. All these observations are the same for three BCs. The first vibration mode shape of three porous FG microbeams is plotted in Fig. 8. It can be seen that these modes exhibit strong triply coupling between axial, bending and shear components.

5. Conclusion

Based on the MSGT with three MLSPs, a quasi-3D theory for FG porous microbeams is presented. The equations of motion are constructed by employing the Lagrange's equations. The verification of the present model is performed, and then parametric study are carried out to investigate the effects of small size, variable MLSP, porosity distribution, gradient index, and boundary conditions on the responses of FG porous microbeams. The results obtained from constant MLSP are significantly different from those from variable one. Three MLSPs in the MSGT should be considered and they need to be variable with the thickness, porosity coefficient and gradient index for the accuracy analysis of FG microbeams especially for very small scale. Some new results for both models constant and variable MLSP of FG porous microbeams are given and can be as a benchmark for future studies.

References

[1] Lü C, Lim C, Chen W. Size-dependent elastic behavior of FGM ultra-thin films based on generalized refined theory. Int J Solids Struct 2009;46(5):1176–85.
[2] Shaat M, Mahmoud F, Alieldin S, Alshorbagy A. Finite element analysis of functionally graded nano-scale films. Finite Elem Anal Des 2013;74:41–52.
[3] Fu Y, Du H, Huang W, Zhang S, Hu M. TiNi-based thin films in MEMS applications: a review. Sensors and Actuators A: Physical. 2004;112(2-3):395-408. doi:10.1016/j.sna.2004.02.019
[4] Lee Z, Ophus C, Fischer L et al. Metallic NEMS components fabricated from nanocomposite Al–Mo films. Nanotechnology. 2006;17(12):3063-3070. doi:10.1088/0957-4484/17/12/042
[5] Baughman R. Carbon Nanotube Actuators. Science. 1999;284(5418):1340-1344. doi:10.1126/science.284.5418.1340
[6] Lau K, Cheung H, Lu J, Yin Y, Hui D, Li H. Carbon Nanotubes for Space and Bio-Engineering Applications. Journal of Computational and Theoretical Nanoscience. 2008;5(1):23-35. doi:10.1166/jctn.2008.003
[7] Rahaeifard M, Kahrobaiyan MH, Ahmadian MT. Sensitivity analysis of atomic force microscope cantilever made of functionally graded materials. ASME 2009 International Design Engineering Technical Conferences and Computers and Information in Engineering Conference 2009:539-544.
[8] Witvrouw A, Mehta A. The Use of Functionally Graded Poly-SiGe Layers for MEMS Applications. Materials Science Forum. 2005;492-493:255-260. doi:10.4028/www.scientific.net/msf.492-493.255
[9] Fleck N, Muller G, Ashby M, Hutchinson J. Strain gradient plasticity: Theory and experiment. Acta Metallurgica et Materialia. 1994;42(2):475-487. doi:10.1016/0956-7151(94)90502-9
[10] Stölken J, Evans A. A microbend test method for measuring the plasticity length scale. Acta Mater. 1998;46(14):5109-5115. doi:10.1016/s1359-6454(98)00153-0
[11] Lam D, Yang F, Chong A, Wang J, Tong P. Experiments and theory in strain gradient elasticity. J Mech Phys Solids. 2003;51(8):1477-1508. doi:10.1016/s0022-5096(03)00053-x
[12] Cosserat E, Cosserat F. Theory of deformable bodies. 1967;Washington, D.C.: National Aeronautics and Space Administration.
[13] Eringen A. Simple microfluids. Int J Eng Sci. 1964;2(2):205-217. doi:10.1016/0020-7225(64)90005-9
[14] Suhubi E, Eringen A. Nonlinear theory of micro-elastic solids—II. Int J Eng Sci. 1964;2(4):389-404. doi:10.1016/0020-7225(64)90017-5
[15] Eringen A. Micropolar fluids with stretch. Int J Eng Sci. 1969;7(1):115-127. doi:10.1016/0020-7225(69)90026-3
[16] Neff P, Forest S. A Geometrically Exact Micromorphic Model for Elastic Metallic Foams Accounting for Affine Microstructure. Modelling, Existence of Minimizers, Identification of Moduli and Computational Results. J Elast. 2007;87(2-3):239-276. doi:10.1007/s10659-007-9106-4
[17] Kröner E. Elasticity theory of materials with long range cohesive forces. Int J Solids Struct. 1967;3(5):731-742. doi:10.1016/0020-7683(67)90049-2
[18] Eringen A. Linear theory of nonlocal elasticity and dispersion of plane waves. Int J Eng Sci. 1972;10(5):425-435. doi:10.1016/0020-7225(72)90050-x
[19] Eringen A. Nonlocal polar elastic continua. Int J Eng Sci. 1972;10(1):1-16. doi:10.1016/0020-7225(72)90070-5
[20] Eringen A, Edelen D. On nonlocal elasticity. Int J Eng Sci. 1972;10(3):233-248. doi:10.1016/0020-7225(72)90039-0
[21] Mindlin R. Micro-structure in linear elasticity. Arch Ration Mech Anal. 1964;16(1):51-78. doi:10.1007/bf00248490

[22] Mindlin R. Second gradient of strain and surface-tension in linear elasticity. Int J Solids Struct. 1965;1(4):417-438. doi:10.1016/0020-7683(65)90006-5
[23] Toupin R. Elastic materials with couple-stresses. Arch Ration Mech Anal. 1962;11(1):385-414. doi:10.1007/bf00253945
[24] Toupin R. Theories of elasticity with couple-stress. Arch Ration Mech Anal. 1964;17(2):85-112. doi:10.1007/bf00253050
[25] Mindlin R, Tiersten H. Effects of couple-stresses in linear elasticity. Arch Ration Mech Anal. 1962;11(1):415-448. doi:10.1007/bf00253946
[26] Koiter WT. Couple stresses in the theory of elasticity. I and II Proc K Ned Akad Wet, 1964;B(67):17–44.
[27] Yang F, Chong A, Lam D, Tong P. Couple stress-based strain gradient theory for elasticity. Int J Solids Struct. 2002;39(10):2731-2743. doi:10.1016/s0020-7683(02)00152-x
[28] Thai H-T, Vo TP, Nguyen TK, Kim S. A review of continuum mechanics models for size-dependent analysis of beams and plates. Compos Struct. 2017;177:196-219. doi:10.1016/j.compstruct.2017.06.040
[29] Shu J, Fleck N. The prediction of a size effect in microindentation. Int J Solids Struct. 1998;35(13):1363-1383. doi:10.1016/s0020-7683(97)00112-1
[30] Kong S, Zhou S, Nie Z, Wang K. Static and dynamic analysis of micro beams based on strain gradient elasticity theory. Int J Eng Sci. 2009;47(4):487-498. doi:10.1016/j.ijengsci.2008.08.008
[31] Wang B, Zhao J, Zhou S. A micro scale Timoshenko beam model based on strain gradient elasticity theory. European Journal of Mechanics - A/Solids. 2010;29(4):591-599. doi:10.1016/j.euromechsol.2009.12.005
[32] Akgöz B, Civalek Ö. A size-dependent shear deformation beam model based on the strain gradient elasticity theory. Int J Eng Sci. 2013;70:1-14. doi:10.1016/j.ijengsci.2013.04.004
[33] Kahrobaiyan M, Asghari M, Ahmadian M. Strain gradient beam element. Finite Elements in Analysis and Design. 2013;68:63-75. doi:10.1016/j.finel.2012.12.006
[34] Wang B, Liu M, Zhao J, Zhou S. A size-dependent Reddy–Levinson beam model based on a strain gradient elasticity theory. Meccanica. 2014;49(6):1427-1441. doi:10.1007/s11012-014-9912-2
[35] Zhang B, He Y, Liu D, Gan Z, Shen L. Non-classical Timoshenko beam element based on the strain gradient elasticity theory. Finite Elements in Analysis and Design. 2014;79:22-39. doi:10.1016/j.finel.2013.10.004
[36] Wang B, Zhou S, Zhao J, Chen X. A size-dependent Kirchhoff micro-plate model based on strain gradient elasticity theory. European Journal of Mechanics - A/Solids. 2011;30(4):517-524. doi:10.1016/j.euromechsol.2011.04.001
[37] Ashoori Movassagh A, Mahmoodi M. A micro-scale modeling of Kirchhoff plate based on modified strain-gradient elasticity theory. European Journal of Mechanics - A/Solids. 2013;40:50-59. doi:10.1016/j.euromechsol.2012.12.008
[38] Wang B, Huang S, Zhao J, Zhou S. Reconsiderations on boundary conditions of Kirchhoff micro-plate model based on a strain gradient elasticity theory. Appl Math Model. 2016;40(15-16):7303-7317. doi:10.1016/j.apm.2016.03.014
[39] Zhang B, Li H, Kong L, Shen H, Zhang X. Size-dependent static and dynamic analysis of Reddy-type micro-beams by strain gradient differential quadrature finite element method. Thin-Walled Structures. 2019:106496. doi:10.1016/j.tws.2019.106496
[40] Ansari R, Gholami R, Sahmani S. Free vibration analysis of size-dependent functionally graded microbeams based on the strain gradient Timoshenko beam theory. Compos Struct. 2011;94(1):221-228. doi:10.1016/j.compstruct.2011.06.024
[41] Ansari R, Gholami R, Faghih Shojaei M, Mohammadi V, Sahmani S. Size-dependent bending, buckling and free vibration of functionally graded Timoshenko microbeams based on the most

general strain gradient theory. Compos Struct. 2013;100:385-397. doi:10.1016/j.compstruct.2012.12.048
[42] Sahmani S, Bahrami M, Ansari R. Nonlinear free vibration analysis of functionally graded third-order shear deformable microbeams based on the modified strain gradient elasticity theory. Compos Struct. 2014;110:219-230. doi:10.1016/j.compstruct.2013.12.004
[43] Akgöz B, Civalek Ö. A new trigonometric beam model for buckling of strain gradient microbeams. International Journal of Mechanical Sciences. 2014;81:88-94. doi:10.1016/j.ijmecsci.2014.02.013
[44] Lei J, He Y, Zhang B, Gan Z, Zeng P. Bending and vibration of functionally graded sinusoidal microbeams based on the strain gradient elasticity theory. International Journal of Engineering Science 2013;72(0):36 – 52.
[45] Sahmani S, Ansari R. On the free vibration response of functionally graded higher-order shear deformable microplates based on the strain gradient elasticity theory. Compos Struct. 2013;95:430-442. doi:10.1016/j.compstruct.2012.07.025
[46] Zhang B, He Y, Liu D, Lei J, Shen L, Wang L. A size-dependent third-order shear deformable plate model incorporating strain gradient effects for mechanical analysis of functionally graded circular/annular microplates. Composites Part B: Engineering. 2015;79:553-580. doi:10.1016/j.compositesb.2015.05.017
[47] Ansari R, Gholami R, Faghih Shojaei M, Mohammadi V, Sahmani S. Bending, buckling and free vibration analysis of size-dependent functionally graded circular/annular microplates based on the modified strain gradient elasticity theory. European Journal of Mechanics - A/Solids. 2015;49:251-267. doi:10.1016/j.euromechsol.2014.07.014
[48] Thai S, Thai HT, Vo TP, Patel V. Size-dependant behaviour of functionally graded microplates based on the modified strain gradient elasticity theory and isogeometric analysis. Computers & Structures. 2017;190:219-241. doi:10.1016/j.compstruc.2017.05.014
[49] Thai S, Thai HT, Vo TP, Nguyen-Xuan H. Nonlinear static and transient isogeometric analysis of functionally graded microplates based on the modified strain gradient theory. Eng Struct. 2017;153:598-612. doi:10.1016/j.engstruct.2017.10.002
[50] Thai C, Ferreira A, Nguyen-Xuan H. Isogeometric analysis of size-dependent isotropic and sandwich functionally graded microplates based on modified strain gradient elasticity theory. Compos Struct. 2018;192:274-288. doi:10.1016/j.compstruct.2018.02.060
[51] Farzam A, Hassani B. Size-dependent analysis of FG microplates with temperature-dependent material properties using modified strain gradient theory and isogeometric approach. Composites Part B: Engineering. 2019;161:150-168. doi:10.1016/j.compositesb.2018.10.028
[52] Zhang B, He Y, Liu D, Shen L, Lei J. Free vibration analysis of four-unknown shear deformable functionally graded cylindrical microshells based on the strain gradient elasticity theory. Compos Struct. 2015;119:578-597. doi:10.1016/j.compstruct.2014.09.032
[53] Barati, M., and A. Zenkour. 2017a. Investigating Post-Buckling Of Geometrically Imperfect Metal Foam Nanobeams With Symmetric And Asymmetric Porosity Distributions. *Composite Structures* 182: 91-98. doi:10.1016/j.compstruct.2017.09.008
[54] Faleh, N., R. Ahmed, and R. Fenjan. 2018. On Vibrations Of Porous FG Nanoshells. *International Journal Of Engineering Science* 133: 1-14. doi:10.1016/j.ijengsci.2018.08.007.
[55] She, G., F. Yuan, Y. Ren, H. Liu, and W. Xiao. 2018. Nonlinear Bending And Vibration Analysis Of Functionally Graded Porous Tubes Via A Nonlocal Strain Gradient Theory. *Composite Structures* 203: 614-623. doi:10.1016/j.compstruct.2018.07.063.

[56] Kim, J., K. Żur, and J. Reddy. 2019. Bending, Free Vibration, And Buckling Of Modified Couples Stress-Based Functionally Graded Porous Micro-Plates. *Composite Structures* 209: 879-888. doi:10.1016/j.compstruct.2018.11.023.
[57] Shojaeefard, M., H. Saeidi Googarchin, M. Ghadiri, and M. Mahinzare. 2017. Micro Temperature-Dependent FG Porous Plate: Free Vibration And Thermal Buckling Analysis Using Modified Couple Stress Theory With CPT And FSDT. *Applied Mathematical Modelling* 50: 633-655. doi:10.1016/j.apm.2017.06.022
[58] Shafiei N, Kazemi M. Buckling analysis on the bi-dimensional functionally graded porous tapered nano-/micro-scale beams. Aerosp Sci Technol 2017;66:1-11
[59] Shafiei N, Mirjavadi SS, Mohasel Afshari B, Rabby S, Kazemi M. Vibration of two-dimensional imperfect functionally graded (2D-FG) porous nano-/micro-beams. Comput Methods Appl Mech Engrg 2017;322:615-32.
[60] Karamanli A, Aydogdu M. Size dependent flapwise vibration analysis of rotating two-directional functionally graded sandwich porous microbeams based on a transverse shear and normal deformation theory. *International Journal of Mechanical Sciences*. 2019;159:165-181. doi:10.1016/j.ijmecsci.2019.05.047
[61] Karamanli A, Aydogdu M. Vibration of functionally graded shear and normal deformable porous microplates via finite element method. *Compos Struct*. 2020;237:111934. doi:10.1016/j.compstruct.2020.111934
[62] Wang Y, Zhao H, Ye C, Zu J. A Porous Microbeam Model for Bending and Vibration Analysis Based on the Sinusoidal Beam Theory and Modified Strain Gradient Theory. International Journal of Applied Mechanics. 2018;10(05):1850059. doi:10.1142/s175882511850059x
[63] Arani A, Zarei H, Pourmousa P. Free Vibration Response of FG Porous Sandwich Micro-Beam with Flexoelectric Face-Sheets Resting on Modified Silica Aerogel Foundation. International Journal of Applied Mechanics. 2019;11(09):1950087. doi:10.1142/s175882511950087x
[64] Asghari M, Ahmadian M, Kahrobaiyan M, Rahaeifard M. On the size-dependent behavior of functionally graded micro-beams. Materials & Design (1980-2015). 2010;31(5):2324-2329. doi:10.1016/j.matdes.2009.12.006
[65] Mindlin R, Influence of couple-stresses on stress concentrations. Wear. 1963;6(3):244. doi:10.1016/0043-1648(63)90084-x
[66] Kahrobaiyan M, Rahaeifard M, Tajalli S, Ahmadian M. A strain gradient functionally graded Euler–Bernoulli beam formulation. Int J Eng Sci. 2012;52:65-76. doi:10.1016/j.ijengsci.2011.11.010
[67] Aghazadeh R, Cigeroglu E, Dag S. Static and free vibration analyses of small-scale functionally graded beams possessing a variable length scale parameter using different beam theories. European Journal of Mechanics - A/Solids. 2014;46:1-11. doi:10.1016/j.euromechsol.2014.01.002
[68] Al-Basyouni K, Tounsi A, Mahmoud S. Size dependent bending and vibration analysis of functionally graded micro beams based on modified couple stress theory and neutral surface position. Compos Struct. 2015;125:621-630. doi:10.1016/j.compstruct.2014.12.070
[69] Chen X, Lu Y, Li Y. Free vibration, buckling and dynamic stability of bi-directional FG microbeam with a variable length scale parameter embedded in elastic medium. Appl Math Model. 2019;67:430-448. doi:10.1016/j.apm.2018.11.004
[70] Thanh C, Tran L, Bui T, Nguyen H, Abdel-Wahab M. Isogeometric analysis for size-dependent nonlinear thermal stability of porous FG microplates. Compos Struct. 2019;221:110838. doi:10.1016/j.compstruct.2019.04.010
[71] Trinh LC, Nguyen HX, Vo TP, Nguyen T-K. Size-dependent behaviour of functionally graded microbeams using various shear deformation theories based on the modified couple stress theory. Compos Struct. 2016; 154:556-572. Doi: 10.1016/j.compstruct.2016.07.033.

[72] Karamanli A, Aydogdu M. Structural dynamics and stability analysis of 2D-FG microbeams with two-directional porosity distribution and variable material length scale parameter. Mechanics Based Design of Structures and Machines. 2020;48(2):164-191. doi: 10.1080/15397734.2019.1627219
[73] Karamanli A, Vo TP. Size-dependent behaviour of functionally graded sandwich microbeams based on the modified strain gradient theory. Compos Struct. 2020; doi.org/10.1016/j.compstruct.2020.112401

Table 1. Verification studies on the deflections of S-S FG microbeams under uniform load for various p_z and h/ℓ_m $(L/h = 10,\ \ell_c = \ell_m = \ell)$

p_z	Reference	Poisson's effect	Theory	h/ℓ_m =1	2	4	8
0.3	Present ($\varepsilon_z \neq 0$)	✓	CCT	0.3620	0.3620	0.3620	0.3620
			MCST	0.0579	0.1565	0.2725	0.3345
			MSGT	0.0246	0.0806	0.1901	0.2935
		-	CCT	0.3834	0.3834	0.3834	0.3834
			MCST	0.0584	0.1603	0.2844	0.3527
			MSGT	0.0247	0.0811	0.1939	0.3056
	Karamanli and Vo [73] (TBT, $\varepsilon_z = 0$)	-	CCT	0.3394	0.3394	0.3394	0.3394
			MCST	0.0571	0.1518	0.2593	0.3150
			MSGT	0.0189	0.0646	0.1642	0.2678
	Lei et al. [44] (SBT, $\varepsilon_z = 0$)	✓	CCT	0.3401	0.3401	0.3401	0.3401
			MCST	0.0571	0.1520	0.2597	0.3157
			MSGT	0.0186	0.0640	0.1635	0.2677
1	Present ($\varepsilon_z \neq 0$)	✓	CCT	0.5260	0.5260	0.5260	0.5260
			MCST	0.0882	0.2347	0.4014	0.4882
			MSGT	0.0375	0.1218	0.2831	0.4311
		-	CCT	0.5739	0.5739	0.5739	0.5739
			MCST	0.0894	0.2437	0.4287	0.5291
			MSGT	0.0376	0.1231	0.2927	0.4592
	Karamanli and Vo [73] (TBT, $\varepsilon_z = 0$)		CCT	0.3394	0.3394	0.3394	0.3394
			MCST	0.0868	0.2261	0.3781	0.4545
			MSGT	0.0287	0.0977	0.2439	0.3899
	Lei et al. [44] (SBT, $\varepsilon_z = 0$)	✓	CCT	0.4872	0.4872	0.4872	0.4872
			MCST	0.0867	0.2260	0.3779	0.4543
			MSGT	0.0284	0.0967	0.2425	0.3890
4	Present ($\varepsilon_z \neq 0$)	✓	CCT	0.7055	0.7055	0.7055	0.7055
			MCST	0.1423	0.3541	0.5649	0.6641
			MSGT	0.0619	0.1935	0.4201	0.6013
		-	CCT	0.7761	0.7761	0.7761	0.7761
			MCST	0.1449	0.3711	0.6094	0.7264
			MSGT	0.0621	0.1964	0.4385	0.6474
	Karamanli and Vo [73] (TBT, $\varepsilon_z = 0$)	-	CCT	0.3394	0.3394	0.3394	0.3394
			MCST	0.1386	0.3341	0.5179	0.6014
			MSGT	0.0472	0.1546	0.3573	0.5318
	Lei et al. [44] (SBT, $\varepsilon_z = 0$)	✓	CCT	0.6353	0.6353	0.6353	0.6353
			MCST	0.1385	0.3341	0.5179	0.6012
			MSGT	0.0467	0.1531	0.3552	0.5306

Table 2. Verification studies on the fundamental frequencies of S-S FG microbeams for various p_z ($L/h = 10, h/\ell_m = 2,\ \ell_c = \ell_m = \ell$)

Reference	Poisson's effect	Theory	$p_z = 0$	0.1	0.6	1.2	2	10
Present ($\varepsilon_z \neq 0$)	✓	CCT	0.5658	0.4996	0.3970	0.3624	0.3446	0.3027
		MCST	0.8505	0.7569	0.6012	0.5391	0.5013	0.4204
		MSGT	1.1806	1.0519	0.8370	0.7465	0.6880	0.5627
	-	CCT	0.5578	0.4895	0.3824	0.3462	0.3281	0.2896
		MCST	0.8453	0.7505	0.5918	0.5283	0.4900	0.4111
		MSGT	1.1791	1.0498	0.8333	0.7419	0.6829	0.5585
Karamanli and Vo [73] (TBT, $\varepsilon_z = 0$)	-	CCT	0.5776	0.5137	0.4114	0.3771	0.3602	0.3235
		MCST	0.8592	0.7671	0.6116	0.5499	0.5131	0.4369
		MSGT	1.3134	1.1744	0.9356	0.8340	0.7686	0.6331
Lei et al. [44] (SBT, $\varepsilon_z = 0$)	✓	CCT	0.5776	0.5129	0.4118	0.3776	0.3607	0.3237
		MCST	0.8592	0.7666	0.6123	0.5508	0.5139	0.4371
		MSGT	1.3210	1.1804	0.9412	0.8392	0.7734	0.6369
Ansari et al. [40] (FBT, $\varepsilon_z = 0$)	✓	CCT	0.5776	0.5129	0.4121	0.3783	0.3617	0.3248
		MCST	0.8538	0.7619	0.6084	0.5470	0.5100	0.4332
		MSGT	1.2608	1.1276	0.8976	0.7986	0.7346	0.6033

Table 3. Verification studies on the deflections of S-S FG microbeams under uniform load with constant and variable MLSP ($L/h = 10$)

h/ℓ_m	Reference	With Poisson's effect				Without Poisson's effect			
		$p_z = 0.3$	1	3	10	$p_z = 0.3$	1	3	10
1	Trinh et al. [71] (Q3D TBT, MCST, $\ell_c = \ell_m$)	0.0579	0.0882	0.1304	0.1776	0.0584	0.0894	0.1328	0.1807
	Present (Q3D TBT, MCST, $\ell_c = \ell_m$)	0.0579	0.0882	0.1304	0.1778	0.0584	0.0894	0.1328	0.1809
	Present (Q3D TBT, MSGT $\ell_c = \ell_m$)	0.0246	0.0375	0.0564	0.0781	0.0247	0.0376	0.0566	0.0784
	Present (Q3D TBT, MCST, $\ell_c \neq \ell_m$)	0.0313	0.0536	0.0927	0.1498	0.0315	0.0540	0.0938	0.1520
	Present (Q3D TBT, MSGT, $\ell_c \neq \ell_m$)	0.0128	0.0218	0.0385	0.0641	0.0128	0.0219	0.0386	0.0643
2	Trinh et al. [71] (Q3D TBT, MCST, $\ell_c = \ell_m$)	0.1565	0.2347	0.3291	0.4333	0.1603	0.2437	0.3447	0.4530
	Present (Q3D TBT, MCST, $\ell_c = \ell_m$)	0.1565	0.2347	0.3291	0.4336	0.1603	0.2437	0.3447	0.4533
	Present (Q3D TBT, MSGT $\ell_c = \ell_m$)	0.0806	0.1218	0.1777	0.2419	0.0811	0.1231	0.1803	0.2454
	Present (Q3D TBT, MCST, $\ell_c \neq \ell_m$)	0.0995	0.1641	0.2616	0.3891	0.1010	0.1684	0.2713	0.4048
	Present (Q3D TBT, MSGT, $\ell_c \neq \ell_m$)	0.0457	0.0768	0.1298	0.2066	0.0458	0.0772	0.1311	0.2091
4	Trinh et al. [71] (Q3D TBT, MCST, $\ell_c = \ell_m$)	0.2726	0.4014	0.5322	0.6777	0.2845	0.4287	0.5745	0.7275
	Present (Q3D TBT, MCST, $\ell_c = \ell_m$)	0.2725	0.4014	0.5322	0.6784	0.2844	0.4287	0.5745	0.7282
	Present (Q3D TBT, MSGT $\ell_c = \ell_m$)	0.1901	0.2830	0.3913	0.5143	0.1939	0.2926	0.4083	0.5356
	Present (Q3D TBT, MCST, $\ell_c \neq \ell_m$)	0.2182	0.3390	0.4816	0.6489	0.2257	0.3582	0.5160	0.6944
	Present (Q3D TBT, MSGT, $\ell_c \neq \ell_m$)	0.1301	0.2098	0.3236	0.4703	0.1316	0.2145	0.3344	0.4875
8	Trinh et al. [71] (Q3D TBT, MCST, $\ell_c = \ell_m$)	0.3346	0.4882	0.6297	0.7894	0.3529	0.5291	0.6897	0.8578
	Present (Q3D TBT, MCST, $\ell_c = \ell_m$)	0.3345	0.4882	0.6297	0.7902	0.3527	0.5291	0.6898	0.8586
	Present (Q3D TBT, MSGT $\ell_c = \ell_m$)	0.2935	0.4310	0.5672	0.7215	0.3055	0.4591	0.6111	0.7731
	Present (Q3D TBT, MCST, $\ell_c \neq \ell_m$)	0.3108	0.4623	0.6106	0.7798	0.3264	0.4988	0.6669	0.8464
	Present (Q3D TBT, MSGT, $\ell_c \neq \ell_m$)	0.2476	0.3787	0.5259	0.6979	0.2552	0.3988	0.5620	0.7453

Table 4. Verification studies on the critical buckling loads of S-S FG microbeams with constant and variable MLSP ($L/h = 10$)

h/ℓ_m	Reference	With Poisson's effect				Without Poisson's effect			
		$p_z = 0$	0.5	1	10	$p_z = 0$	0.5	1	10
1	Trinh et al. [71] (Q3D TBT, MCST, $\ell_c = \ell_m$)	-	-	-	-	365.2609	186.3476	144.0387	71.2964
	Present (Q3D TBT, MCST, $\ell_c = \ell_m$)	367.0178	188.4132	146.1060	72.5777	365.2609	186.3597	144.0387	71.2466
	Present (Q3D TBT, MSGT $\ell_c = \ell_m$)	862.4540	444.7685	344.5813	165.6321	861.9055	443.8952	343.6299	164.9945
	Present (Q3D TBT, MCST, $\ell_c \neq \ell_m$)	749.8015	333.9865	240.6000	86.1031	748.0447	331.9322	238.5292	84.7679
	Present (Q3D TBT, MSGT, $\ell_c \neq \ell_m$)	1854.7341	824.1687	592.5424	201.8396	1854.2192	823.3312	591.6196	201.2021
2	Trinh et al. [71] (Q3D TBT, MCST, $\ell_c = \ell_m$)	-	-	-	-	135.5906	67.7727	52.8346	28.4424
	Present (Q3D TBT, MCST, $\ell_c = \ell_m$)	137.3475	69.8334	54.8990	29.7447	135.5906	67.7800	52.8346	28.4192
	Present (Q3D TBT, MSGT $\ell_c = \ell_m$)	265.8818	135.9651	106.0980	53.4194	265.1764	134.9075	104.9555	52.6455
	Present (Q3D TBT, MCST, $\ell_c \neq \ell_m$)	233.0435	106.2277	78.5355	33.1562	231.2866	104.1738	76.4678	31.8268
	Present (Q3D TBT, MSGT, $\ell_c \neq \ell_m$)	514.8534	231.1752	168.3796	62.5639	514.2605	230.2205	167.3261	61.8085
4	Trinh et al. [71] (Q3D TBT, MCST, $\ell_c = \ell_m$)	-	-	-	-	78.1731	38.1289	30.0290	17.7049
	Present (Q3D TBT, MCST, $\ell_c = \ell_m$)	79.9299	40.1883	32.0910	19.0086	78.1731	38.1351	30.0290	17.6885
	Present (Q3D TBT, MSGT $\ell_c = \ell_m$)	114.3608	57.6644	45.5832	25.0985	113.2871	56.2302	44.0747	24.0833
	Present (Q3D TBT, MCST, $\ell_c \neq \ell_m$)	103.8539	49.2872	38.0052	19.8729	102.0971	47.2337	35.9414	18.5506
	Present (Q3D TBT, MSGT, $\ell_c \neq \ell_m$)	178.0703	81.9893	61.5239	27.4225	177.2376	80.7500	60.1764	26.4677
8	Trinh et al. [71] (Q3D TBT, MCST, $\ell_c = \ell_m$)	-	-	-	-	63.6316	30.1391	23.7487	14.8532
	Present (Q3D TBT, MCST, $\ell_c = \ell_m$)	65.5756	32.7770	26.3875	16.3166	63.8187	30.7236	24.3265	14.9990
	Present (Q3D TBT, MSGT $\ell_c = \ell_m$)	74.7154	37.3499	29.9024	17.8752	73.2394	35.5412	28.0531	16.6662
	Present (Q3D TBT, MCST, $\ell_c \neq \ell_m$)	71.5566	35.0518	27.8668	16.5344	69.7997	32.9985	25.8053	15.2161
	Present (Q3D TBT, MSGT, $\ell_c \neq \ell_m$)	91.4886	43.6852	34.3442	18.4838	90.2305	42.0296	32.3109	17.2919

Table 5. Verification studies on the fundamental frequencies of S-S FG microbeams with constant and variable MLSP ($L/h = 10$)

h/ℓ_m	Reference	With Poisson's effect				Without Poisson's effect			
		$p_z = 0.3$	1	3	10	$p_z = 0.3$	1	3	10
1	Trinh et al. [71] (Q3D TBT, MCST, $\ell_c = \ell_m$)	12.7422	10.5093	8.7936	7.6236	12.6894	10.4388	8.7161	7.5587
	Present (Q3D TBT, MCST, $\ell_c = \ell_m$)	12.7328	10.4908	8.7796	7.6172	12.6780	10.4156	8.6975	7.5506
	Present (Q3D TBT, MSGT $\ell_c = \ell_m$)	19.5006	16.0705	13.3455	11.4897	19.4806	16.0361	13.3075	11.4638
	Present (Q3D TBT, MCST, $\ell_c \neq \ell_m$)	17.2960	13.4566	10.4140	8.2958	17.2562	13.3956	10.3432	8.2350
	Present (Q3D TBT, MSGT, $\ell_c \neq \ell_m$)	27.0588	21.0312	16.1395	12.6810	27.0122	20.9705	16.0923	12.6554
2	Trinh et al. [71] (Q3D TBT, MCST, $\ell_c = \ell_m$)	7.7504	6.4429	5.5363	4.8816	7.6582	6.3231	5.4091	4.7749
	Present (Q3D TBT, MCST, $\ell_c = \ell_m$)	7.7458	6.4330	5.5286	4.8774	7.6527	6.3110	5.3992	4.7700
	Present (Q3D TBT, MSGT $\ell_c = \ell_m$)	10.7860	8.9278	7.5218	6.5288	10.7520	8.8763	7.4630	6.4809
	Present (Q3D TBT, MCST, $\ell_c \neq \ell_m$)	9.7113	7.6933	6.2011	5.1492	9.6380	7.5914	6.0854	5.0475
	Present (Q3D TBT, MSGT, $\ell_c \neq \ell_m$)	14.3276	11.2422	8.8006	7.0644	14.3034	11.2018	8.7511	7.0209
4	Trinh et al. [71] (Q3D TBT, MCST, $\ell_c = \ell_m$)	5.8726	4.9262	4.3533	3.9029	5.7486	4.7672	4.1898	3.7676
	Present (Q3D TBT, MCST, $\ell_c = \ell_m$)	5.8696	4.9189	4.3475	3.8995	5.7449	4.7584	4.1825	3.7636
	Present (Q3D TBT, MSGT $\ell_c = \ell_m$)	7.0263	5.8570	5.0693	4.4781	6.9560	5.7582	4.9605	4.3874
	Present (Q3D TBT, MCST, $\ell_c \neq \ell_m$)	6.5599	5.3527	4.5703	3.9870	6.4490	5.2056	4.4133	3.8541
	Present (Q3D TBT, MSGT, $\ell_c \neq \ell_m$)	8.4907	6.8019	5.5742	4.6827	8.4413	6.7252	5.4813	4.5986
8	Trinh et al. [71] (Q3D TBT, MCST, $\ell_c = \ell_m$)	5.3001	4.4671	4.0022	3.6163	5.1619	4.2908	3.8238	3.4696
	Present (Q3D TBT, MCST, $\ell_c = \ell_m$)	5.2976	4.4605	3.9969	3.6130	5.1588	4.2830	3.8172	3.4658
	Present (Q3D TBT, MSGT $\ell_c = \ell_m$)	5.6550	4.7467	4.2110	3.7808	5.5423	4.5974	4.0551	3.6522
	Present (Q3D TBT, MCST, $\ell_c \neq \ell_m$)	5.4963	4.5838	4.0589	3.6370	5.3628	4.4112	3.8819	3.4908
	Present (Q3D TBT, MSGT, $\ell_c \neq \ell_m$)	6.1569	5.0637	4.3735	3.8443	6.0639	4.9327	4.2284	3.7198

Table 6. Verification studies on the fundamental frequencies of the FG porous microbeams ($\alpha_0 = 0.1, \ell/h = 0.15, \ell_c = \ell_m = \ell$)

L/h	BCs	Theory	Poisson's effect	FGM I				FGM II			
				$p_z = 0$	1	5	10	$p_z = 0$	1	5	10
12	C-C	Present (Q3D TBT, MSGT)	✓	26.3981	17.7939	14.5987	13.8740	25.9952	18.0404	14.9844	14.2869
		Present (Q3D TBT, MCST)	✓	24.2721	16.4371	13.5750	12.9163	23.9939	16.7406	13.9797	13.3422
		Present (Q3D TBT, MSGT)	-	26.0088	17.3406	14.1661	13.4504	25.5101	17.4819	14.4479	13.7602
		Present (Q3D TBT, MCST)	-	23.7782	15.8842	13.0663	12.4213	23.3926	16.0692	13.3641	12.7421
		Karamanli and Aydogdu [72] (Q3D TBT, MCST)	-	23.7744	15.8815	13.0625	12.4194	-	-	-	-
		Shafiei et al. [59] (FBT, MCST)	-	23.4313	16.0784	13.4679	12.8762	23.1017	16.2674	13.7621	13.1914
	S-S	Present (Q3D TBT, MSGT)	✓	11.9079	8.0587	6.6166	6.2701	11.7231	8.1595	6.7820	6.4509
		Present (Q3D TBT, MCST)	✓	10.9891	7.4831	6.1927	5.8737	10.8657	7.6109	6.3717	6.0659
		Present (Q3D TBT, MSGT)	-	11.7422	7.8832	6.4434	6.0964	11.5184	7.9411	6.5680	6.2365
		Present (Q3D TBT, MCST)	-	10.7678	7.2574	5.9780	5.6598	10.5985	7.3372	6.1127	5.8082
	C-F	Present (Q3D TBT, MSGT)	✓	4.2862	2.8885	2.3785	2.2598	4.2232	2.9318	2.4437	2.3293
		Present (Q3D TBT, MCST)	✓	3.9454	2.6725	2.2193	2.1111	3.9042	2.7256	2.2893	2.1845
		Present (Q3D TBT, MSGT)	-	4.2220	2.8138	2.3063	2.1895	4.1435	2.8391	2.3545	2.2421
		Present (Q3D TBT, MCST)	-	3.8622	2.5798	2.1326	2.0270	3.8032	2.6132	2.1845	2.0826
18	C-C	Present (Q3D TBT, MSGT)	✓	26.9427	18.1584	14.9290	14.1857	26.5408	18.4246	15.3324	14.6165
		Present (Q3D TBT, MCST)	✓	24.7855	16.7889	13.9100	13.2334	24.5179	17.1138	14.3399	13.6846
		Present (Q3D TBT, MSGT)	-	26.5422	17.6925	14.4810	13.7481	26.0427	17.8454	14.7776	14.0731
		Present (Q3D TBT, MCST)	-	24.2696	16.2127	13.3743	12.7130	23.8905	16.4143	13.6918	13.0537
		Karamanli and Aydogdu [72] (Q3D TBT, MCST)	-	24.2657	16.2084	13.3671	12.7092	-	-	-	-
		Shafiei et al. [59] (FBT, MCST)	-	24.0340	16.4872	13.8296	13.2224	23.7081	16.6915	14.1407	13.5548
	S-S	Present (Q3D TBT, MSGT)	✓	11.9816	8.1100	6.6621	6.3131	11.7979	8.2132	6.8304	6.4970
		Present (Q3D TBT, MCST)	✓	11.0541	7.5291	6.2354	5.4191	10.9327	7.6599	6.4179	6.1099
		Present (Q3D TBT, MSGT)	-	11.8135	7.9317	6.4858	6.1363	11.5901	7.9913	6.6124	6.2786
		Present (Q3D TBT, MCST)	-	10.8295	7.3000	6.0168	5.6963	10.6615	7.3819	6.1540	5.8473
	C-F	Present (Q3D TBT, MSGT)	✓	4.2929	2.8921	2.3814	2.2624	4.2294	2.9349	2.4463	2.3316
		Present (Q3D TBT, MCST)	✓	3.9541	2.6779	2.2241	2.1154	3.9127	2.7308	2.2941	2.1888
		Present (Q3D TBT, MSGT)	-	4.2296	2.8185	2.3104	2.1932	4.1508	2.8437	2.3585	2.2459
		Present (Q3D TBT, MCST)	-	3.8712	2.5857	2.1378	2.0319	3.8122	2.6192	2.1899	2.0877

Table 7. Verification studies on the critical buckling loads of C-C FGM I porous microbeams for various p_z and α_0 ($L/h = 40, h/\ell = 5$, $\ell_c = \ell_m = \ell$).

α_0	Theory	Poisson's effect	$p_z = 0$	0.1	0.5	2	6
0	Present (Q3D TBT, MSGT)	✓	62.9538	60.0687	53.1933	45.9920	42.0805
	Present (Q3D TBT, MCST)	✓	49.4530	47.2808	42.1386	37.0580	34.3182
	Present (Q3D TBT, MSGT)	-	61.0667	58.0760	50.8879	43.4068	39.5586
	Present (Q3D TBT, MCST)	-	46.9867	44.7025	39.2451	33.9363	31.3245
	Karamanli and Aydogdu [72] (Q3D TBT, MCST)	-	46.9072	44.6636	39.2169	33.9166	31.3078
	Shafiei and Kazemi (CBT, MCST) [58]	-	48.8871	45.1740	40.7701	35.3948	32.6857
0.1	Present (Q3D TBT, MSGT)	✓	58.2258	55.2816	48.2061	40.7907	36.9027
	Present (Q3D TBT, MCST)	✓	45.1704	42.9644	37.6792	32.4571	29.7923
	Present (Q3D TBT, MSGT)	-	56.9405	53.9184	46.6206	39.0066	35.1720
	Present (Q3D TBT, MCST)	-	43.4344	41.1399	35.6192	30.2318	27.6682
	Karamanli and Aydogdu [72] (Q3D TBT, MCST)	-	43.4190	41.1079	35.5980	30.2177	27.6552
	Shafiei and Kazemi (CBT, MCST) [58]	-	43.0365	41.3188	36.8804	31.4834	28.7908

Table 8. DFFs of the FG microbeams for various $p_z, L/h, h/\ell_m$ and BCs with constant and variable MLSP

L/h	h/ℓ_m	DFFs ($\ell_c = \ell_m = \ell$)				DFFs ($\ell_c \neq \ell_m \neq \ell$)			
		$p_z = 0$	1	2	5	$p_z = 0$	1	2	5
S-S									
5	1	19.3717	15.5201	13.7253	11.6983	19.7353	15.7519	13.9402	11.8547
	2	13.0832	9.9522	8.8003	7.5469	18.1904	12.4714	10.6479	8.6483
	4	8.6009	6.4685	5.7323	5.0323	10.7164	7.5239	6.5112	5.4924
	8	6.9666	5.1864	4.6038	4.1268	7.7007	5.5449	4.8663	4.2805
20	1	24.9861	19.2356	16.9132	14.1774	36.6411	25.0046	21.0934	16.6172
	2	13.8740	10.5987	9.3567	7.9804	19.3054	13.2810	11.2910	9.0893
	4	9.1012	6.8590	6.0931	5.3650	11.3549	7.9632	6.8833	5.8015
	8	7.3589	5.4890	4.9018	4.4445	8.1415	5.8642	5.1671	4.5844
C-F									
5	1	8.9863	6.9250	6.1175	5.1572	13.2042	9.0449	7.6782	6.0853
	2	4.9510	3.7902	3.3548	2.8701	6.9263	4.7802	4.0816	3.2970
	4	3.2085	2.4261	2.1553	1.8962	4.0319	2.8347	2.4532	2.0672
	8	2.5741	1.9264	1.7179	1.5509	2.8585	2.0648	1.8178	1.6070
20	1	9.0117	6.9403	6.1028	5.1156	13.2237	9.0257	7.6148	5.9993
	2	4.9916	3.8155	3.3683	2.8725	6.9575	4.7864	4.0688	3.2745
	4	3.2621	2.4606	2.1860	1.9252	4.0789	2.8607	2.4722	2.0832
	8	2.6313	1.9644	1.7548	1.5922	2.9144	2.1002	1.8508	1.6427
C-C									
5	1	45.0532	35.1904	30.8780	26.3406	52.9570	36.8976	31.4557	26.5225
	2	27.3269	21.0727	18.9837	16.5348	38.3329	26.9790	23.6928	19.6154
	4	17.5800	13.4216	11.9753	10.4620	22.1937	15.8703	13.9387	11.7880
	8	13.9920	10.5816	9.3687	8.1800	15.6081	11.4242	10.0459	8.6572
20	1	56.9719	43.9072	38.7404	32.5959	83.6303	57.2435	48.5083	38.3623
	2	31.5109	24.1112	21.3303	18.2302	43.9651	30.3223	25.8628	20.8686
	4	20.5453	15.5192	13.7917	12.1373	25.7252	18.0784	15.6457	13.1869
	8	16.5471	12.3711	11.0415	9.9829	18.3415	13.2394	11.6634	10.3243

Table 9. DCBLs of the FG microbeams for various $p_z, L/h, h/\ell_m$ and BCs with constant and variable MLSP

L/h	h/ℓ_m	DCBLs ($\ell_c = \ell_m = \ell$)				DCBLs ($\ell_c \neq \ell_m \neq \ell$)			
		$p_z = 0$	1	2	5	$p_z = 0$	1	2	5
S-S									
5	1	134.0166	74.6510	57.5872	40.4256	288.2347	127.9029	91.4005	56.6786
	2	41.2953	22.6906	17.5139	12.6079	79.9924	36.0343	26.0082	16.7392
	4	17.7398	9.5064	7.3455	5.5300	27.6453	12.9051	9.5168	6.6150
	8	11.5727	6.0823	4.7130	3.6956	14.1823	6.9644	5.2752	3.9832
20	1	143.3734	79.5758	60.1431	41.2725	308.3421	134.4788	93.5574	56.7053
	2	44.1949	24.1525	18.4016	13.0733	85.5849	37.9297	26.7997	16.9607
	4	19.0091	10.1114	7.8004	5.9064	29.5980	13.6314	9.9561	6.9071
	8	12.4223	6.4733	5.0468	4.0524	15.2086	7.3893	5.6084	4.3119
C-F									
5	1	36.5239	20.3050	15.4440	10.6748	78.7176	34.5166	24.2177	14.7890
	2	11.1634	6.1189	4.6785	3.3364	21.7450	9.6807	6.8800	4.3727
	4	4.7379	2.5313	1.9535	1.4778	7.4356	3.4369	2.5146	1.7440
	8	3.0687	1.6064	1.2510	0.9999	3.7734	1.8406	1.3960	1.0691
20	1	36.3333	20.1644	15.2272	10.4412	78.1893	34.0745	23.6822	14.3442
	2	11.1719	6.1062	4.6492	3.3011	21.6717	9.5963	6.7735	4.2831
	4	4.7873	2.5473	1.9648	1.4883	7.4704	3.4381	2.5093	1.7402
	8	3.1215	1.6270	1.2689	1.0204	3.8256	1.8584	1.4105	1.0854
C-C									
5	1	472.5783	265.3896	212.8470	156.7963	1021.6446	467.6984	352.9939	231.3832
	2	142.6992	79.5140	63.0316	46.6533	280.2948	130.1261	98.1505	65.6894
	4	59.3518	32.4687	25.2129	18.7465	94.2942	45.2313	34.0575	23.7378
	8	37.8400	20.3648	15.5846	11.6038	46.9034	23.6247	17.8260	12.9195
20	1	576.6000	320.4444	243.4756	168.0632	1241.4884	543.8821	381.0020	232.2976
	2	176.9253	96.8863	74.0402	52.7680	343.7022	152.9021	108.5694	68.9628
	4	75.5569	40.3065	31.1001	23.5239	118.1431	54.5720	39.9238	27.6967
	8	49.1470	25.6881	19.9999	15.9837	60.3050	29.3842	22.2857	17.0689

Table 10. DMDs of the FG microbeams for various $p_z, L/h, h/\ell_m$ and BCs with constant and variable MLSP

L/h	h/ℓ_m	DMDs ($\ell_c = \ell_m = \ell$)				DMDs ($\ell_c \neq \ell_m \neq \ell$)			
		$p_z = 0$	1	2	5	$p_z = 0$	1	2	5
S-S									
5	1	1.9262	3.4584	4.4852	6.3932	0.8961	2.0203	2.8290	4.5650
	2	6.2351	11.3518	14.7069	20.4337	3.2247	7.1595	9.9215	15.4170
	4	14.4392	26.9760	34.8938	46.3422	9.2959	19.9147	26.9909	38.8151
	8	22.0287	41.9983	54.1669	69.0675	18.0201	36.7302	48.4550	64.1462
20	1	1.7659	3.1817	4.2099	6.1350	0.8211	1.8829	2.7065	4.4656
	2	5.7279	10.4813	13.7568	19.3639	2.9581	6.6749	9.4470	14.9273
	4	13.3123	25.0283	32.4423	42.8448	8.5516	18.5680	25.4215	36.6419
	8	20.3646	39.0847	50.1301	62.4306	16.6365	34.2425	45.1138	58.6778
C-F									
5	1	5.9287	10.7425	13.6733	19.5588	2.3763	6.1456	8.6233	13.9269
	2	19.4153	36.8864	46.2626	63.7824	9.9660	22.0825	30.7387	47.8920
	4	46.4214	86.9867	112.4438	148.5461	29.5122	63.1679	85.8366	123.7851
	8	72.9513	138.4534	178.2054	225.6379	58.9856	120.1268	158.4652	208.8158
20	1	5.8371	10.5124	13.9034	20.2404	2.7110	6.2101	8.9201	14.6996
	2	19.0592	34.8395	45.7260	64.3478	9.7986	22.1107	31.2897	49.4455
	4	44.7495	83.9803	108.8764	143.7415	28.5748	62.0491	85.0070	122.6028
	8	68.8916	131.9851	169.2775	210.6502	56.1115	115.3907	152.0749	197.7477
C-C									
5	1	0.4497	0.7963	0.9916	1.3439	0.2046	0.4515	0.5973	0.9092
	2	1.4822	2.6617	3.3493	4.5155	0.7546	1.6235	2.1480	3.2010
	4	3.5699	6.5380	8.3938	11.2671	2.2442	4.6792	6.1951	8.8664
	8	5.6266	10.4974	13.6877	18.4067	4.5252	9.0089	11.9060	16.4332
20	1	0.3491	0.6280	0.8256	1.1944	0.1620	0.3695	0.5267	0.8625
	2	1.1411	2.0823	2.7228	3.8173	0.5862	1.3169	1.8525	2.9139
	4	2.6839	5.0257	6.5112	8.6077	1.7120	3.7040	5.0605	7.2939
	8	4.1373	7.9085	10.1572	12.7199	3.3675	6.9055	9.1036	11.8939

Table 11. DFFs/DCBLs/DMDs of the S-S FG porous microbeams for various $p_z, L/h, h/\ell_m$ and BCs with constant MLSP ($\alpha_0 = 0.1, \ell_c = \ell_m \neq \ell$)

L/h	h/ℓ_m	MCST (FGM I)				MCST (FGM II)				MCST (FGM III)			
		$p_z = 0$	1	2	5	$p_z = 0$	1	2	5	$p_z = 0$	1	2	5
DFF													
5	1	14.7521	11.1974	9.7909	8.0761	15.2460	11.4520	9.9624	8.3592	15.3028	11.5036	9.9536	8.2794
	2	9.2303	7.0253	6.2282	5.2859	9.4257	7.0353	6.1547	5.3097	9.3935	6.9936	6.0813	5.1979
	4	7.2100	5.5018	4.9387	4.2826	7.2672	5.3570	4.6965	4.1545	7.1843	5.2595	4.5867	4.0356
	8	6.6086	5.0484	4.5562	3.9829	6.6178	4.8461	4.2518	3.8023	6.5154	4.7260	4.1274	3.6844
20	1	15.3186	11.6403	10.1740	8.3923	15.8258	12.0266	10.5377	8.8637	15.9095	12.0923	10.5247	8.7628
	2	9.6319	7.3401	6.5283	5.5774	9.8349	7.3788	6.4892	5.6337	9.8030	7.3302	6.4035	5.5029
	4	7.5698	5.7825	5.2252	4.6034	7.6349	5.6478	4.9873	4.4739	7.5395	5.5323	4.8541	4.3186
	8	6.9594	5.3212	4.8417	4.3229	6.9774	5.1245	4.5347	4.1329	6.8579	4.9824	4.3820	3.9674
DCBLs													
5	1	46.9473	24.5469	17.8997	11.7676	52.8906	28.6020	21.5370	14.9066	53.8902	29.1752	21.6908	14.7196
	2	18.3309	9.2426	6.7026	4.6449	20.1542	10.6506	8.0432	5.8625	20.2497	10.6500	7.9418	5.6800
	4	11.1767	5.4155	3.9026	2.8444	11.9692	6.1627	4.6650	3.5651	11.8382	6.0148	4.5045	3.4075
	8	9.3882	4.4585	3.2024	2.3885	9.9227	5.0408	3.8193	2.9787	9.7351	4.8552	3.6452	2.8359
20	1	48.7739	25.4088	18.4322	12.0744	54.7727	29.5326	22.1423	15.2847	56.1153	30.2957	22.4197	15.1681
	2	19.2828	9.6498	6.9893	4.8834	21.1528	11.1167	8.3963	6.1742	21.3050	11.1322	8.2990	5.9814
	4	11.9100	5.7100	4.1286	3.0841	12.7477	6.5127	4.9595	3.8937	12.6023	6.3410	4.7688	3.6838
	8	10.0668	4.7251	3.4134	2.6338	10.6464	5.3617	4.1002	3.3226	10.4266	5.1432	3.8863	3.1091
DMDs													
5	1	5.4126	10.3681	14.2187	21.6627	4.8112	8.9152	11.8434	17.1432	4.7164	8.7274	11.7423	17.3354
	2	13.8570	27.5325	37.9539	54.8194	12.6196	23.9334	31.6912	43.5338	12.5492	23.9094	32.0599	44.8795
	4	22.7161	46.9772	65.1479	89.3957	21.2370	41.3438	54.5961	71.4653	21.4584	42.3294	56.4977	74.7200
	8	27.0369	57.0507	79.3667	106.3742	25.6087	50.5328	66.6555	85.4439	26.0885	52.4325	69.7970	89.7184
20	1	5.1855	9.9550	13.7223	20.9491	4.6180	8.5659	11.4246	16.5517	4.5072	8.3496	11.2825	16.6776
	2	13.1159	26.2118	36.1875	51.7949	11.9574	22.7555	30.1274	40.9725	11.8714	22.7228	30.4790	42.2904
	4	21.2347	44.2965	61.2609	82.0077	19.8408	38.8410	51.0036	64.9647	20.0690	39.8912	53.0402	68.6644
	8	25.1224	53.5299	74.0959	96.0252	23.7564	47.1783	61.6917	76.1280	24.2564	49.1814	65.0844	81.3544

Table 12. DFFs of the FGM I porous microbeams for various $p_z, L/h, h/\ell_m$ and BCs with constant and variable MLSP ($\alpha_0 = 0.1$)

L/h	h/ℓ_m	MSGT ($\ell_c = \ell_m = \ell$)				MSGT ($\ell_c = \ell_m \neq \ell$)				MSGT ($\ell_c \neq \ell_m \neq \ell$)			
		$p_z = 0$	1	2	5	$p_z = 0$	1	2	5	$p_z = 0$	1	2	5
S-S													
5	1	19.5607	15.2234	13.1466	10.7220	19.4776	14.9885	12.8750	10.4786	19.8472*	15.3674*	13.2684*	10.7790*
	2	13.4570	9.9766	8.6305	7.1364	12.4576	9.2201	7.9766	6.6175	17.3750	11.5972	9.7073	7.6272
	4	8.8206	6.4220	5.5343	4.6842	8.4288	6.1162	5.2653	4.4729	10.4353	7.1031	5.9973	4.9015
	8	7.1111	5.0800	4.3511	3.7622	6.9835	4.9791	4.2618	3.6936	7.6709	5.3134	4.5102	3.8379
20	1	25.7211	19.4025	16.7708	13.5886	23.3611	17.6038	15.2188	12.3517	34.7026	23.0798	19.1725	14.6463
	2	14.2684	10.6435	9.2108	7.5905	13.2048	9.8233	8.5018	7.0338	18.4361	12.3510	10.3247	8.0736
	4	9.3299	6.8111	5.8893	5.0060	8.9120	6.4831	5.6034	4.7881	11.0511	7.5169	6.3511	5.2003
	8	7.5062	5.3738	4.6335	4.0613	7.3701	5.2659	4.5390	3.9919	8.1035	5.6162	4.7921	4.1252
C-F													
5	1	9.2493	6.9841	6.0676	4.9479	8.3939	6.3325	5.5012	4.4920	12.5006	8.3495	6.9802	5.3640
	2	5.0895	3.8048	3.3019	2.7299	4.7016	3.5059	3.0415	2.5229	6.6063	4.4411	3.7276	2.9228
	4	3.2865	2.4072	2.0817	1.7676	3.1342	2.2877	1.9770	1.6864	3.9152	2.6701	2.2578	1.8466
	8	2.6238	1.8846	1.6231	1.4157	2.5747	1.8456	1.5888	1.3898	2.8401	1.9741	1.6830	1.4423
20	1	9.2764	7.0008	6.0522	4.9042	8.4231	6.3503	5.4907	4.4564	12.5225	8.3303	6.9216	5.2884
	2	5.1328	3.8311	3.3155	2.7317	4.7474	3.5340	3.0586	2.5300	6.6416	4.4494	3.7191	2.9071
	4	3.3430	2.4425	2.1121	1.7955	3.1917	2.3237	2.0086	1.7167	3.9669	2.6982	2.2792	1.8657
	8	2.6832	1.9223	1.6580	1.4543	2.6341	1.8834	1.6239	1.4293	2.8990	2.0100	1.7152	1.4772
C-C													
5	1	45.7426	34.5904	29.5447	24.1490	44.3569	33.7824	28.9693	23.6955	51.7457	35.1215	29.2895	23.6996
	2	28.1009	21.2098	18.8107	15.9375	25.9371	19.5400	17.2942	14.6547	36.5513	25.1611	21.7724	17.5439
	4	18.0266	13.3850	11.6802	9.8908	17.1717	12.7124	11.0638	9.3647	21.5453	15.0131	12.9147	10.6096
	8	14.2914	10.4285	8.9659	7.5639	14.0109	10.2045	8.7598	7.3853	15.5167	10.9876	9.3928	7.8317
20	1	58.6434	44.2940	38.4401	31.2886	53.2411	40.1738	34.8646	28.4194	79.1899	52.8536	44.1193	33.8440
	2	32.3994	24.2130	21.0058	17.3544	29.9570	22.3295	19.3678	16.0575	41.9594	28.1917	23.6452	18.5314
	4	21.0530	15.4079	13.3323	11.3287	20.0937	14.6545	12.6728	10.8203	25.0083	17.0503	14.4241	11.8080
	8	16.8730	12.1102	10.4406	9.1245	16.5619	11.8631	10.2234	8.9623	18.2396	12.6716	10.8133	9.2847

* Denote axial mode, the rest are flexural mode

Table 13. DCBLs of the FGM I porous microbeams for various $p_z, L/h, h/\ell_m$ and BCs with constant and variable MLSP ($\alpha_0 = 0.1$)

L/h	h/ℓ_m	MSGT ($\ell_c = \ell_m = \ell$)				MSGT ($\ell_c = \ell_m \neq \ell$)				MSGT ($\ell_c \neq \ell_m \neq \ell$)			
		$p_z = 0$	1	2	5	$p_z = 0$	1	2	5	$p_z = 0$	1	2	5
S-S													
5	1	128.7274	68.4265	51.0432	33.5513	106.1837	56.3421	42.0110	27.6808	234.3447	98.3923	68.1474	39.7030
	2	39.5901	20.6302	15.3072	10.3038	33.9017	17.5782	13.0231	8.8135	66.1201	28.1335	19.6068	11.8889
	4	16.8985	8.4586	6.1948	4.3463	15.4135	7.6637	5.5997	3.9560	23.7308	10.3775	7.3010	4.7766
	8	10.9139	5.2627	3.8048	2.7803	10.5188	5.0528	3.6483	2.6781	12.7320	5.7654	4.0938	2.8979
20	1	137.7134	72.8849	53.1129	33.9732	113.5986	59.9958	43.7351	28.0680	250.6931	103.1388	69.4216	39.4703
	2	42.3681	21.9263	16.0154	10.5965	36.2846	18.6761	13.6438	9.0985	70.7440	29.5289	20.1250	11.9890
	4	18.1059	8.9750	6.5444	4.6070	16.5191	8.1308	5.9240	4.2144	25.4090	10.9329	7.6117	4.9719
	8	11.7141	5.5845	4.0496	3.0314	11.2926	5.3624	3.8859	2.9286	13.6550	6.1004	4.3318	3.1277
C-F													
5	1	35.0761	18.5980	13.6504	8.8055	28.9087	15.2981	11.2284	7.2639	63.9724	26.4831	17.9851	10.3054
	2	10.6964	5.5532	4.0727	2.7062	9.1423	4.7218	3.4615	2.3164	17.9498	7.5300	5.1614	3.0860
	4	4.5083	2.2449	1.6380	1.1520	4.1056	2.0302	1.4797	1.0508	6.3670	2.7500	1.9175	1.2511
	8	2.8909	1.3847	1.0034	0.7474	2.7847	1.3285	0.9620	0.7211	3.3806	1.5165	1.0764	0.7736
20	1	34.8973	18.4669	13.4439	8.5906	28.7790	15.1974	11.0675	7.0956	63.5625	26.1260	17.5662	9.9798
	2	10.7086	5.5418	4.0444	2.6735	9.1657	4.7177	3.4438	2.2946	17.9066	7.4663	5.0826	3.0245
	4	4.5585	2.2598	1.6471	1.1596	4.1570	2.0462	1.4904	1.0606	6.4085	2.7548	1.9162	1.2510
	8	2.9427	1.4028	1.0173	0.7625	2.8363	1.3467	0.9760	0.7367	3.4328	1.5329	1.0883	0.7865
C-C													
5	1	453.8503	243.6184	190.1047	132.7147	373.6046	200.3637	156.1113	109.0197	829.8708	361.5962	265.9139	164.8839
	2	136.7417	72.4966	55.5845	38.8518	116.5568	61.5745	47.0034	32.8486	231.0414	101.9263	74.5068	47.1572
	4	56.4996	29.0283	21.5088	14.9814	51.3017	26.2083	19.3141	13.4408	80.5505	36.4339	26.2540	17.2194
	8	35.6726	17.7349	12.7612	8.8425	34.3118	16.9987	12.1963	8.4466	41.9614	19.6317	13.9624	9.4462
20	1	553.7875	293.5351	215.1934	138.6088	456.5990	241.5324	177.0822	114.4023	1009.1380	417.3314	282.9468	161.8705
	2	169.5653	87.9534	64.4691	42.8176	145.0632	74.8470	54.8452	36.6886	283.8948	119.0075	81.5081	48.7213
	4	71.9291	35.7664	26.0949	18.3527	65.5610	32.3728	23.5921	16.7559	101.2844	43.7227	30.4874	19.9035
	8	46.3212	22.1553	16.0514	11.9553	44.6372	21.2654	15.3948	11.5388	54.0829	24.2377	17.2028	12.3663

Table 14. DMDs of the FGM I porous microbeams for various $p_z, L/h, h/\ell_m$ and BCs with constant and variable MLSP ($\alpha_0 = 0.1$)

L/h	h/ℓ_m	MSGT ($\ell_c = \ell_m = \ell$)				MSGT ($\ell_c = \ell_m \neq \ell$)				MSGT ($\ell_c \neq \ell_m \neq \ell$)			
		$p_z = 0$	1	2	5	$p_z = 0$	1	2	5	$p_z = 0$	1	2	5
S-S													
5	1	2.0053	3.7727	5.0599	7.7028	2.4304	4.5808	6.1459	9.3328	1.1021	2.6259	3.7939	6.5155
	2	6.5023	12.4817	16.8201	24.9871	7.5881	14.6398	19.7555	29.1876	3.8996	9.1652	13.1515	21.6839
	4	15.1492	30.2913	41.3284	58.8724	16.5929	33.4056	45.6803	64.6189	10.8179	24.7329	35.1245	53.6341
	8	23.3328	48.4658	66.9751	91.5944	24.1962	50.4560	69.8159	95.0473	20.0426	44.2871	62.3016	87.9372
20	1	1.8385	3.4738	4.7671	7.4531	2.2287	4.2200	5.7892	9.0209	1.0100	2.4550	3.6474	6.4154
	2	5.9747	11.5452	15.8060	23.8888	6.9761	13.5538	18.5526	27.8203	3.5786	8.5735	12.5796	21.1158
	4	13.9758	28.1958	38.6654	54.9232	15.3173	31.1215	42.7119	60.0359	9.9607	23.1490	33.2473	50.8962
	8	21.5942	45.2999	62.4654	83.4428	22.3995	47.1755	65.0947	86.3703	18.5274	41.4724	58.3989	80.8780
C-F													
5	1	5.7852	11.6044	15.4749	23.6227	7.4402	13.9185	18.8389	28.6681	3.8608	7.9962	11.5849	19.9075
	2	20.2760	37.9167	52.0704	78.3927	23.8272	45.2167	61.8302	91.9964	11.9917	28.1921	40.8381	67.8535
	4	48.8141	97.7747	133.9197	190.2123	54.0112	108.5123	148.4486	209.7718	34.3755	79.1779	112.7974	173.2895
	8	77.4764	160.4807	221.6098	301.1630	80.4922	167.4049	231.4784	313.0376	66.0007	145.8591	205.4638	288.8266
20	1	6.0767	11.4800	15.7463	24.5948	7.3732	13.9552	19.1336	29.7952	3.3344	8.1026	12.0259	21.1282
	2	19.8885	38.3969	52.5749	79.4729	23.2578	45.1416	61.8050	92.7051	11.8664	28.4360	41.7302	70.0937
	4	47.0161	94.7160	129.9493	184.6342	51.6000	104.6855	143.7407	202.0689	33.3484	77.5359	111.4717	170.8500
	8	73.1077	153.1681	211.2580	282.0874	75.8708	159.5957	220.2608	292.1136	62.5911	140.0407	197.3093	273.2699
C-C													
5	1	0.4634	0.8673	1.1098	1.5864	0.5645	1.0546	1.3514	1.9310	0.2573	0.5838	0.7926	1.2745
	2	1.5463	2.9157	3.7939	5.4117	1.8136	3.4337	4.4858	6.3992	0.9141	2.0717	2.8266	4.4500
	4	3.7447	7.2955	9.8071	14.0345	4.1257	8.0843	10.9248	15.6533	2.6256	5.8012	8.0159	12.1765
	8	5.9481	11.9910	16.6029	23.9687	6.1878	12.5209	17.3906	25.1386	5.0489	10.8030	15.1264	22.3493
20	1	0.3635	0.6856	0.9340	1.4477	0.4410	0.8334	1.1354	1.7548	0.1994	0.4816	0.7092	1.2376
	2	1.1908	2.2941	3.1271	4.7041	1.3929	2.6974	3.6783	5.4942	0.7100	1.6926	2.4685	4.1263
	4	2.8198	5.6647	7.7605	11.0334	3.0955	6.2619	8.5889	12.0935	1.9985	4.6264	6.6312	10.1577
	8	4.3897	9.1690	12.6524	17.0014	4.5562	9.5549	13.1954	17.6219	3.7567	8.3748	11.7959	16.4212

Table 15. DFFs of the FGM II porous microbeams for various $p_z, L/h, h/\ell_m$ and BCs with constant and variable MLSP ($\alpha_0 = 0.1$)

L/h	h/ℓ_m	MSGT ($\ell_c = \ell_m = \ell$)				MSGT ($\ell_c = \ell_m \neq \ell$)				MSGT ($\ell_c \neq \ell_m \neq \ell$)			
		$p_z = 0$	1	2	5	$p_z = 0$	1	2	5	$p_z = 0$	1	2	5
S-S													
5	1	19.4554	15.3725	13.4462	11.2424	19.4155	15.2839	13.3514	11.1707	19.7822*	15.5555*	13.6161*	11.3650*
	2	13.2848	10.0036	8.7667	7.4148	12.8434	9.6695	8.5029	7.2371	17.8775	12.1310	10.3163	8.3309
	4	8.7346	6.4957	5.6992	4.9446	8.5593	6.3602	5.5925	4.8758	10.6261	7.3852	6.3589	5.3386
	8	7.0734	5.1990	4.5611	4.0421	7.0159	5.1545	4.5263	4.0206	7.7253	5.4997	4.7842	4.1774
20	1	25.3500	19.3370	16.8694	13.9308	24.2199	18.4808	16.1967	13.4781	35.7213	24.1315	20.3394	15.9593
	2	14.0836	10.6557	9.3301	7.8521	13.5730	10.2657	9.0244	7.6500	18.9029	12.8794	10.9339	8.7730
	4	9.2442	6.8920	6.0649	5.2819	9.0436	6.7374	5.9438	5.2047	11.2342	7.8044	6.7202	5.6449
	8	7.4748	5.5080	4.8656	4.3729	7.4097	5.4578	4.8264	4.3489	8.1623	5.8171	5.0858	4.4897
C-F													
5	1	9.1186	6.9654	6.1067	5.0739	8.7284	6.6694	5.8715	4.9131	12.8994	8.7500	7.4181	5.8531
	2	5.0252	3.8110	3.3462	2.8252	4.8471	3.6748	3.2384	2.7531	6.7909	4.6423	3.9566	3.1841
	4	3.2575	2.4366	2.1443	1.8655	3.1870	2.3822	2.1015	1.8380	3.9894	2.7782	2.3945	2.0102
	8	2.6133	1.9317	1.7038	1.5230	2.5905	1.9141	1.6900	1.5145	2.8644	2.0469	1.7877	1.5712
20	1	9.1427	6.9769	6.0873	5.0270	8.7339	6.6672	5.8440	4.8634	12.8905	8.7102	7.3431	5.7627
	2	5.0668	3.8358	3.3586	2.8261	4.8817	3.6945	3.2478	2.7529	6.8111	4.6408	3.9396	3.1602
	4	3.3131	2.4722	2.1757	1.8952	3.2403	2.4161	2.1318	1.8672	4.0343	2.8028	2.4130	2.0264
	8	2.6726	1.9711	1.7418	1.5666	2.6491	1.9529	1.7276	1.5579	2.9212	2.0829	1.8213	1.6086
C-C													
5	1	45.3710	34.9169	30.2696	25.3521	44.6959	34.4647	29.9497	25.1315	52.3515	35.9450	30.3814	25.2407
	2	27.7703	21.2580	19.0396	16.4221	26.9885	20.6539	18.5415	16.0673	37.9333	26.5059	23.2305	19.1577
	4	17.8504	13.4989	11.9486	10.3250	17.5332	13.2499	11.7470	10.1882	22.0884	15.6646	13.7050	11.5393
	8	14.1958	10.6110	9.2955	7.9938	14.0900	10.5275	9.2287	7.9494	15.6702	11.3524	9.9049	8.4472
20	1	57.8147	44.1649	38.6748	32.0708	55.3073	42.2618	37.1672	31.0452	81.6528	55.3439	46.8501	36.8967
	2	31.9887	24.2479	21.2805	17.9510	30.8488	23.3761	20.5926	17.4924	43.0935	29.4409	25.0709	20.1599
	4	20.8650	15.5927	13.7284	11.9492	20.4150	15.2453	13.4554	11.7743	25.4586	17.7233	15.2792	12.8330
	8	16.8044	12.4114	10.9578	9.8144	16.6586	12.2987	10.8697	9.7602	18.3859	13.1312	11.4784	10.1050

* Denote axial mode, the rest are flexural mode

Table 16. DCBLs of the FGM II porous microbeams for various $p_z, L/h, h/\ell_m$ and BCs with constant and variable MLSP ($\alpha_0 = 0.1$)

L/h	h/ℓ_m	MSGT ($\ell_c = \ell_m = \ell$)				MSGT ($\ell_c = \ell_m \neq \ell$)				MSGT ($\ell_c \neq \ell_m \neq \ell$)			
		$p_z = 0$	1	2	5	$p_z = 0$	1	2	5	$p_z = 0$	1	2	5
S-S													
5	1	131.7529	71.9633	54.6792	37.2959	121.3247	66.2947	50.7365	35.0486	263.7561	114.5121	81.4760	49.9800
	2	40.6104	21.8498	16.5969	11.6440	37.9593	20.4071	15.6018	11.0838	73.7184	32.5050	23.3427	14.8934
	4	17.4480	9.1269	6.9187	5.0895	16.7494	8.7483	6.6608	4.9480	25.9210	11.8392	8.6520	5.9618
	8	11.3762	5.8172	4.4058	3.3756	11.1896	5.7172	4.3385	3.3396	13.6077	6.5206	4.8565	3.6131
20	1	140.7290	76.4367	56.8088	37.7916	128.4607	69.8169	52.3680	35.3749	279.4517	119.0520	82.5937	49.6040
	2	43.4265	23.2044	17.3723	12.0026	40.3333	21.5364	16.2519	11.3926	78.2440	33.9041	23.8604	14.9843
	4	18.7007	9.7034	7.3376	5.4291	17.8973	9.2726	7.0472	5.2714	27.6262	12.4444	9.0099	6.2014
	8	12.2218	6.1954	4.7210	3.7203	12.0097	6.0830	4.6452	3.6795	14.5763	6.9108	5.1584	3.9217
C-F													
5	1	35.8657	19.5242	14.6099	9.7961	32.8177	17.8758	13.4920	9.1790	71.5480	30.6608	21.4432	12.9695
	2	10.9700	5.8811	4.4200	3.0664	10.1998	5.4647	4.1381	2.9114	19.9181	8.6718	6.1361	3.8681
	4	4.6594	2.4284	1.8372	1.3578	4.4596	2.3209	1.7645	1.3182	6.9425	3.1385	2.2758	1.5654
	8	3.0178	1.5366	1.1695	0.9164	2.9653	1.5087	1.1507	0.9062	3.6149	1.7205	1.2832	0.9709
20	1	35.6602	19.3655	14.3795	9.5575	32.5369	17.6810	13.2513	8.9447	70.8329	30.1514	20.8995	12.5447
	2	10.9768	5.8654	4.3879	3.0294	10.1898	5.4413	4.1034	2.8747	19.8033	8.5732	6.0276	3.7822
	4	4.7093	2.4442	1.8478	1.3676	4.5054	2.3349	1.7742	1.3276	6.9694	3.1371	2.2696	1.5616
	8	3.0710	1.5571	1.1868	0.9368	3.0173	1.5286	1.1676	0.9265	3.6656	1.7375	1.2969	0.9871
C-C													
5	1	465.8384	257.4747	204.2239	147.2129	435.4037	240.7891	191.9986	139.6409	950.3422	427.7802	321.6194	208.5646
	2	140.5194	76.9027	60.2008	43.6548	132.7322	72.6117	57.1060	41.7959	261.8018	119.4290	89.6569	59.4937
	4	58.3347	31.2009	23.8169	17.2988	56.2716	30.0616	23.0216	16.8454	89.0518	41.8746	31.2565	21.5656
	8	37.1225	19.4468	14.5499	10.4917	36.5711	19.1443	14.3448	10.3793	45.0596	22.1578	16.4393	11.6491
20	1	566.1780	308.0843	230.2820	154.1810	517.8987	281.9767	212.6021	144.4448	1127.9044	482.8563	337.1695	203.6172
	2	173.8675	93.1232	69.9497	48.4998	161.6708	86.5310	65.4918	46.0518	314.7752	136.9414	96.8169	61.0027
	4	74.3151	38.6742	29.2537	21.6187	71.1449	36.9698	28.1023	20.9918	110.3361	49.8477	36.1446	24.8709
	8	48.3378	24.5757	18.7004	14.6517	47.5022	24.1313	18.4010	14.4907	57.7897	27.4752	20.4915	15.5072

Table 17. DMDs of the FGM II porous microbeams for various $p_z, L/h, h/\ell_m$ and BCs with constant and variable MLSP ($\alpha_0 = 0.1$)

L/h	h/ℓ_m	MSGT ($\ell_c = \ell_m = \ell$)				MSGT ($\ell_c = \ell_m \neq \ell$)				MSGT ($\ell_c \neq \ell_m \neq \ell$)			
		$p_z = 0$	1	2	5	$p_z = 0$	1	2	5	$p_z = 0$	1	2	5
S-S													
5	1	1.9594	3.5878	4.7241	6.9305	2.1281	3.8952	5.0917	7.3752	0.9795	2.2571	3.1743	5.1776
	2	6.3398	11.7876	15.5175	22.1210	6.7820	12.6201	16.5056	23.2364	3.4993	7.9370	11.0539	17.3250
	4	14.6776	28.0887	37.0311	50.3243	15.2852	29.2968	38.4562	51.7529	9.9113	21.6992	29.6744	43.0411
	8	22.4019	43.8904	57.9078	75.5477	22.7710	44.6513	58.7988	76.3546	18.7714	39.2058	52.5960	70.6549
20	1	1.7991	3.3124	4.4570	6.7001	1.9709	3.6265	4.8350	7.1578	0.9061	2.1269	3.0658	5.1049
	2	5.8292	10.9094	14.5718	21.0910	6.2762	11.7543	15.5762	22.2201	3.2357	7.4674	10.6107	16.8959
	4	13.5316	26.0801	34.4873	46.6102	14.1388	27.2913	35.9079	48.0036	9.1617	20.3386	28.0901	40.8096
	8	20.6982	40.8361	53.5867	68.0003	21.0636	41.5905	54.4608	68.7533	17.3575	36.6118	49.0469	64.5110
C-F													
5	1	6.3985	10.9374	14.4384	21.2384	6.6989	11.8876	15.5550	22.6281	2.9001	6.8746	9.6769	15.8091
	2	19.8776	36.4160	47.9826	69.4036	21.2004	39.4830	51.2640	72.7693	10.7797	24.3264	34.3460	53.8682
	4	47.4622	90.4265	119.3865	161.5393	49.7202	94.5343	124.4334	166.6735	31.0934	69.0958	94.5636	137.4756
	8	74.2293	144.7810	190.7088	246.8859	75.5126	147.4313	193.7987	249.6640	61.5157	128.4856	172.3841	230.2973
20	1	5.9462	10.9448	14.7195	22.1056	6.5151	11.9821	15.9630	23.6125	2.9898	7.0151	10.1000	16.7989
	2	19.3986	36.2683	48.4456	70.1123	20.8957	39.0920	51.8045	73.8913	10.7195	24.7408	35.1539	55.9883
	4	45.4972	87.5399	115.7925	156.4739	47.5643	91.6501	120.6156	161.2077	30.6339	68.0170	94.0081	136.6746
	8	70.0345	137.9468	181.0256	229.5553	71.2853	140.5245	184.0117	232.1301	58.5763	123.4552	165.4464	217.5583
C-C													
5	1	0.4564	0.8206	1.0332	1.4307	0.4843	0.8772	1.0986	1.5078	0.2216	0.4934	0.6552	1.0079
	2	1.5045	2.7494	3.5046	4.8211	1.5923	2.9111	3.6928	5.0337	0.8068	1.7678	2.3494	3.5304
	4	3.6308	6.7961	8.8733	12.1886	3.7625	7.0511	9.1770	12.5149	2.3745	5.0485	6.7399	9.7422
	8	5.7302	10.9755	14.6316	20.3105	5.8159	11.1491	14.8422	20.5364	4.7057	9.5905	12.8858	18.1854
20	1	0.3555	0.6531	0.8727	1.3015	0.3885	0.7133	0.9449	1.3889	0.1783	0.4160	0.5948	0.9835
	2	1.1612	2.1663	2.8817	4.1524	1.2486	2.3311	3.0776	4.3731	0.6399	1.4698	2.0768	3.2932
	4	2.7289	5.2380	6.9221	9.3663	2.8506	5.4796	7.2059	9.6466	1.8332	4.0550	5.5895	8.1228
	8	4.2067	8.2666	10.8629	13.8785	4.2806	8.4189	11.0398	14.0332	3.5143	7.3856	9.9008	13.0936

Table 18. DFFs of the FGM III porous microbeams for various $p_z, L/h, h/\ell_m$ and BCs with constant and variable MLSP ($\alpha_0 = 0.1$)

L/h	h/ℓ_m	MSGT ($\ell_c = \ell_m = \ell$)				MSGT ($\ell_c = \ell_m \neq \ell$)				MSGT ($\ell_c \neq \ell_m \neq \ell$)			
		$p_z = 0$	1	2	5	$p_z = 0$	1	2	5	$p_z = 0$	1	2	5
S-S													
5	1	19.4302	15.4147	13.5280	11.3704	19.4020	15.3489	13.4375	11.2701	19.7679	15.6267	13.7168	11.4858
	2	13.1837	9.9213	8.7038	7.3691	12.7925	9.6244	8.4180	7.1009	17.8116	12.0791	10.1955	8.1220
	4	8.6427	6.4027	5.6111	4.8566	8.4923	6.2860	5.4960	4.7481	10.5648	7.3129	6.2442	5.1729
	8	6.9729	5.0859	4.4485	3.9344	6.9245	5.0481	4.4110	3.8994	7.6447	5.3995	4.6648	4.0403
20	1	25.2201	19.2719	16.8496	13.9702	24.4057	18.6444	16.2350	13.3817	35.9521	24.2837	20.2519	15.6313
	2	13.9836	10.5782	9.2705	7.8100	13.6153	10.2918	8.9898	7.5449	18.9825	12.9121	10.8492	8.5677
	4	9.1407	6.7858	5.9617	5.1752	8.9955	6.6713	5.8491	5.0719	11.2176	7.7530	6.6135	5.4771
	8	7.3577	5.3743	4.7275	4.2258	7.3101	5.3367	4.6905	4.1930	8.0826	5.7071	4.9501	4.3240
C-F													
5	1	9.0676	6.9326	6.0900	5.0787	8.7490	6.6877	5.8524	4.8533	12.9194	8.7591	7.3548	5.7135
	2	4.9887	3.7809	3.3222	2.8072	4.8449	3.6695	3.2134	2.7046	6.7925	4.6352	3.9123	3.0998
	4	3.2216	2.3995	2.1083	1.8286	3.1655	2.3554	2.0650	1.7884	3.9747	2.7544	2.3520	1.9465
	8	2.5734	1.8861	1.6572	1.4755	2.5553	1.8718	1.6431	1.4626	2.8346	2.0076	1.7399	1.5143
20	1	9.0960	6.9536	6.0801	5.0410	8.8020	6.7269	5.8579	4.8279	12.9752	8.7655	7.3108	5.6428
	2	5.0307	3.8078	3.3371	2.8109	4.8974	3.7042	3.2354	2.7149	6.8405	4.6528	3.9088	3.0856
	4	3.2756	2.4337	2.1383	1.8564	3.2230	2.3922	2.0975	1.8191	4.0285	2.7842	2.3744	1.9657
	8	2.6303	1.9228	1.6918	1.5131	2.6132	1.9091	1.6784	1.5013	2.8925	2.0431	1.7722	1.5486
C-C													
5	1	45.2765	34.9596	30.4063	25.5868	44.7987	34.7313	30.2249	25.4030	52.5273	36.3611	30.7288	25.5022
	2	27.5055	20.9903	18.7870	16.1815	26.4629	20.1872	18.0000	15.4315	37.1869	25.8924	22.5149	18.3157
	4	17.6650	13.3085	11.7667	10.1555	17.2627	12.9964	11.4536	9.8467	21.7283	15.3485	13.3177	11.0657
	8	14.0222	10.4214	9.1216	7.8841	13.8922	10.3198	9.0184	7.7794	15.4511	11.1290	9.6565	8.2065
20	1	57.4870	43.9648	38.5767	32.1099	55.5269	42.4551	37.1070	30.7117	81.8986	55.4871	46.5048	36.0472
	2	31.7514	24.0559	21.1274	17.8364	30.8674	23.3697	20.4562	17.2030	43.1538	29.4303	24.8140	19.6427
	4	20.6301	15.3512	13.4936	11.7083	20.2843	15.0793	13.2259	11.4605	25.3803	17.5806	15.0150	12.4328
	8	16.5429	12.1133	10.6521	9.4977	16.4307	12.0244	10.5645	9.4187	18.1964	12.8784	11.1696	9.7353

Table 19. DCBLs of the FGM III porous microbeams for various $p_z, L/h, h/\ell_m$ and BCs with constant and variable MLSP ($\alpha_0 = 0.1$)

L/h	h/ℓ_m	MSGT ($\ell_c = \ell_m = \ell$)				MSGT ($\ell_c = \ell_m \neq \ell$)				MSGT ($\ell_c \neq \ell_m \neq \ell$)			
		$p_z = 0$	1	2	5	$p_z = 0$	1	2	5	$p_z = 0$	1	2	5
S-S													
5	1	131.7746	72.0364	54.9356	37.7365	122.1042	66.7226	50.5299	34.3616	265.2472	115.0785	80.5498	48.0496
	2	40.5212	21.7739	16.5580	11.6280	38.1246	20.4610	15.4555	10.7690	74.0739	32.5763	22.9898	14.2484
	4	17.3041	8.9872	6.7946	4.9739	16.6973	8.6571	6.5134	4.7492	25.9468	11.7576	8.4432	5.6612
	8	11.1942	5.6404	4.2462	3.2426	11.0362	5.5553	4.1735	3.1838	13.4940	6.3676	4.6761	3.4239
20	1	141.2208	77.0482	57.5341	38.5948	132.2460	72.1112	53.4124	35.4104	286.9952	122.3440	83.1236	48.3215
	2	43.4044	23.2073	17.4108	12.0582	41.1472	21.9669	16.3718	11.2531	79.9974	34.5811	23.8480	14.5123
	4	18.5370	9.5457	7.1970	5.2924	17.9522	9.2261	6.9276	5.0832	27.9258	12.4630	8.8580	5.9283
	8	12.0050	5.9854	4.5241	3.5277	11.8503	5.9018	4.4534	3.4731	14.4904	6.7503	4.9606	3.6938
C-F													
5	1	35.9527	19.6369	14.7588	9.9743	33.5463	18.3136	13.6566	9.1247	72.9918	31.2841	21.4523	12.5729
	2	10.9577	5.8747	4.4233	3.0750	10.3569	5.5448	4.1469	2.8605	20.2557	8.7966	6.1035	3.7298
	4	4.6178	2.3884	1.8016	1.3236	4.4644	2.3046	1.7309	1.2683	6.9971	3.1345	2.2315	1.4923
	8	2.9644	1.4849	1.1215	0.8709	2.9242	1.4631	1.1031	0.8565	3.5898	1.6792	1.2333	0.9148
20	1	35.7895	19.5259	14.5674	9.7635	33.5265	18.2810	13.5271	8.9590	72.8065	31.0106	21.0443	12.2228
	2	10.9717	5.8669	4.3984	3.0441	10.4022	5.5539	4.1362	2.8410	20.2615	8.7502	6.0272	3.6639
	4	4.6676	2.4041	1.8121	1.3328	4.5202	2.3235	1.7442	1.2802	7.0477	3.1426	2.2317	1.4929
	8	3.0160	1.5038	1.1368	0.8875	2.9771	1.4827	1.1190	0.8738	3.6441	1.6969	1.2468	0.9292
C-C													
5	1	463.2175	254.5774	201.9618	145.8190	421.2805	231.4936	182.4084	130.5066	922.1476	412.2451	305.6204	193.5256
	2	139.7492	76.0957	59.4958	43.0228	129.4213	70.4204	54.6318	39.1283	255.0344	115.6188	85.4247	55.1439
	4	57.8954	30.7721	23.4438	16.9959	55.3417	29.3768	22.2338	15.9924	87.4092	40.8231	29.9698	20.1413
	8	36.6620	19.0052	14.1993	10.3517	36.0160	18.6548	13.8950	10.0937	44.4175	21.6081	15.8588	11.1701
20	1	567.6585	309.9751	232.7256	157.0700	530.0340	289.2794	215.4920	143.7902	1151.9834	493.3052	337.7237	197.6178
	2	173.6959	93.0433	70.0195	48.6494	164.2882	87.8770	65.6923	45.2930	320.3978	139.0464	96.3948	58.8811
	4	73.6616	38.0455	28.6938	21.0800	71.2506	36.7286	27.5821	20.2108	111.2605	49.8134	35.4622	23.7262
	8	47.4896	23.7542	17.9362	13.9271	46.8574	23.4121	17.6469	13.7011	57.4060	26.8267	19.7027	14.6174

Table 20. DMDs of the FGM III porous microbeams for various p_z, L/h and BCs with constant and variable MLSP ($\alpha_0 = 0.1$)

L/h	h/ℓ_m	MSGT ($\ell_c = \ell_m = \ell$)				MSGT ($\ell_c = \ell_m \neq \ell$)				MSGT ($\ell_c \neq \ell_m \neq \ell$)			
		$p_z = 0$	1	2	5	$p_z = 0$	1	2	5	$p_z = 0$	1	2	5
S-S													
5	1	1.9589	3.5835	4.7010	6.8477	2.1132	3.8674	5.1089	7.5174	0.9735	2.2445	3.2089	5.3828
	2	6.3534	11.8275	15.5521	22.1481	6.7497	12.5812	16.6537	23.9018	3.4808	7.9156	11.2180	18.0994
	4	14.7977	28.5215	37.7021	51.4865	15.3289	29.5976	39.3122	53.8948	9.8988	21.8436	30.3964	45.3015
	8	22.7590	45.2510	60.0654	78.6352	23.0796	45.9351	61.0983	80.0654	18.9249	40.1348	54.6014	74.5258
20	1	1.7928	3.2861	4.4008	6.5606	1.9144	3.5110	4.7402	7.1504	0.8822	2.0695	3.0462	5.2402
	2	5.8321	10.9080	14.5395	20.9934	6.1519	11.5236	15.4617	22.4947	3.1647	7.3210	10.6160	17.4449
	4	13.6510	26.5108	35.1607	47.8129	14.0954	27.4284	36.5272	49.7793	9.0633	20.3079	28.5712	42.6882
	8	21.0716	42.2680	55.9181	71.7118	21.3464	42.8665	56.8043	72.8364	17.4602	37.4816	51.0012	68.4896
C-F													
5	1	6.2519	10.7901	14.2998	20.9620	6.6472	11.4801	15.5196	23.0253	3.1310	6.8455	9.7944	16.4383
	2	19.8437	35.8813	49.3244	68.9526	21.6871	40.9646	50.7881	74.8646	10.5198	24.1290	34.6458	56.4214
	4	47.6520	91.8692	121.6863	165.9261	49.6327	95.6163	127.1444	173.8027	31.1219	69.2855	97.1918	145.1241
	8	75.5104	149.6351	198.4271	258.1408	76.6377	152.0428	201.9943	263.1077	62.1048	131.8018	179.4208	244.0597
20	1	5.9263	10.8582	14.5371	21.6523	6.3329	11.6095	15.6689	23.6122	2.9136	6.8338	10.0486	17.2624
	2	19.4107	36.2704	48.3478	69.8037	20.4905	38.3456	51.4564	74.8650	10.4898	24.2713	35.1971	57.8634
	4	45.9090	89.0129	118.0949	160.5786	47.4323	92.1514	122.7643	167.2955	30.3141	67.9434	95.6743	143.0897
	8	71.3184	142.8473	188.9995	242.2432	72.2649	144.9084	192.0465	246.1095	58.9404	126.4499	172.1470	231.1701
C-C													
5	1	0.4601	0.8302	1.0451	1.4449	0.5015	0.9134	1.1577	1.6151	0.2325	0.5124	0.6902	1.0872
	2	1.5132	2.7799	3.5479	4.8940	1.6343	3.0104	3.8661	5.3838	0.8283	1.8281	2.4686	3.8125
	4	3.6578	6.8916	9.0151	12.4065	3.8296	7.2269	9.5158	13.1982	2.4218	5.1865	7.0385	10.4412
	8	5.7954	11.2164	14.9705	20.5542	5.9044	11.4386	15.3151	21.1115	4.7766	9.8387	13.3589	18.9696
20	1	0.3546	0.6493	0.8639	1.2782	0.5609	1.0452	1.3498	1.9453	0.1747	0.4078	0.5946	1.0144
	2	1.1625	2.1688	2.8798	4.1413	1.7964	3.3863	4.4514	6.4301	0.6293	1.4491	2.0880	3.4154
	4	2.7533	5.3252	7.0581	9.6068	4.0937	7.9590	10.7741	15.5182	1.8192	4.0606	5.7010	8.5212
	8	4.2816	8.5522	11.3244	14.5948	6.1792	12.4556	17.2012	24.4468	3.5389	7.5664	10.2999	13.8923

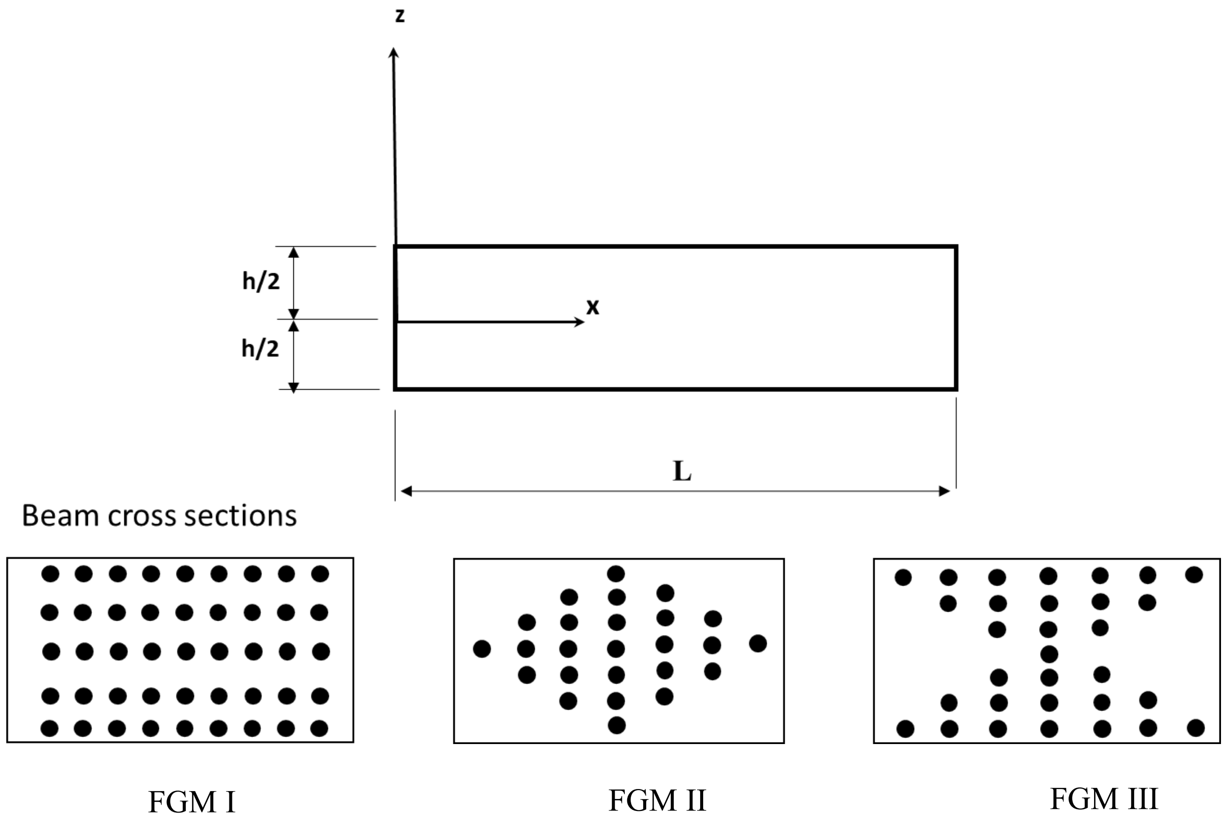

Figure 1. Three FGM models for strain gradient porous microbeams

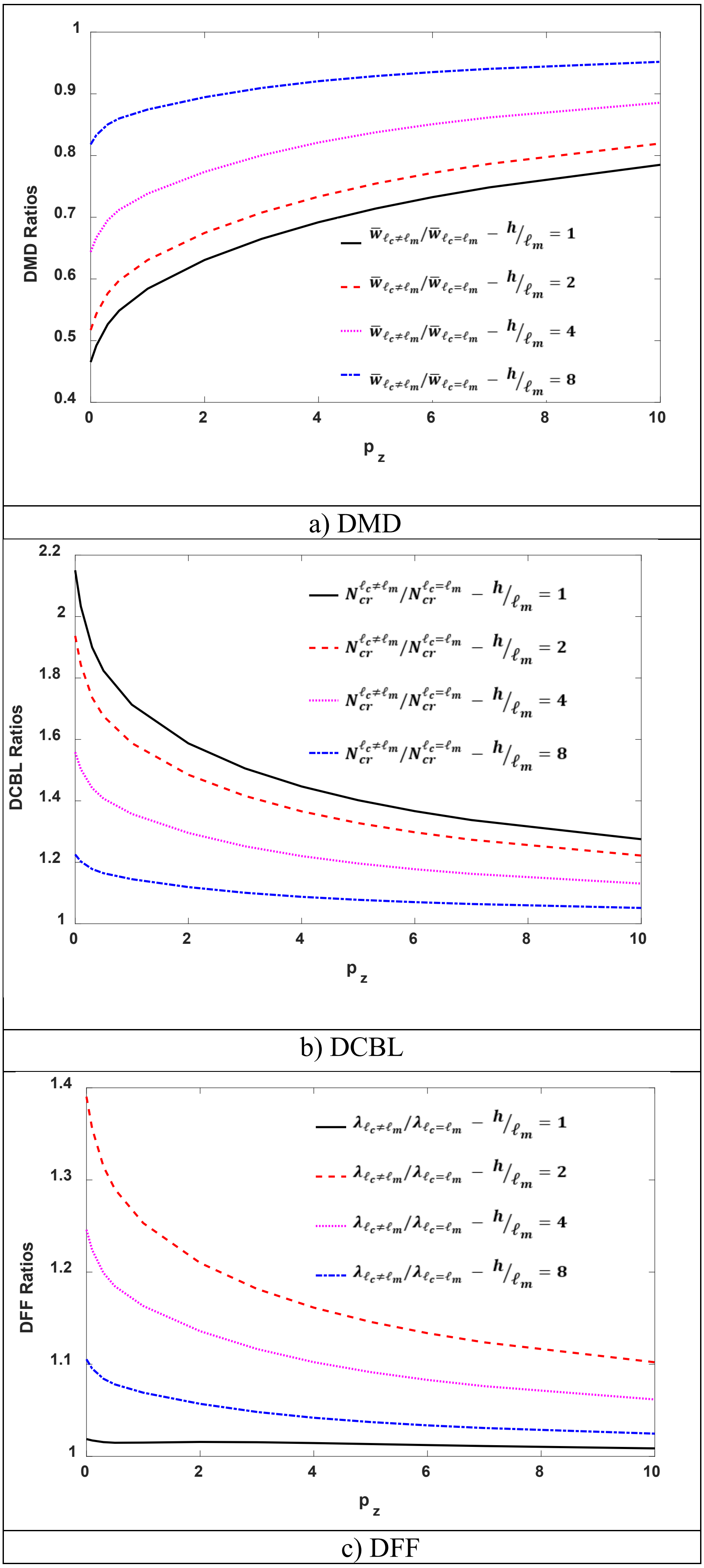

Figure 2. Ratio of DFFs, DCBLs and DMDs of S-S FG microbeams between the results of MSGT obtained from variable MLPS ($\ell_m \neq \ell_c \neq \ell$) and constant MLSP ($\ell_m = \ell_c = \ell$) with respect to p_z ($L/h = 5, h/\ell_m = 1, 2,4,8$)

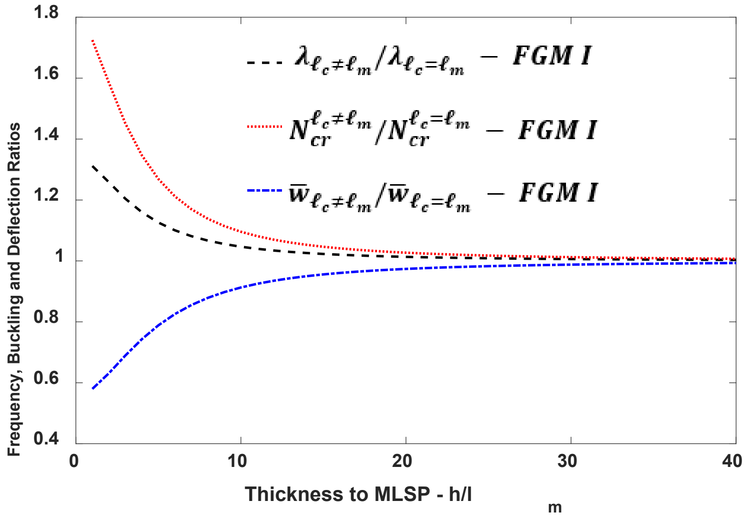

a) FGM I

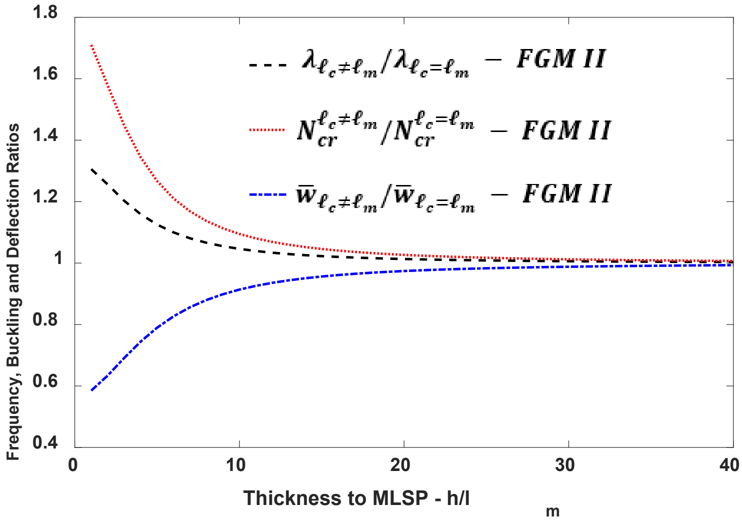

b) FGM II

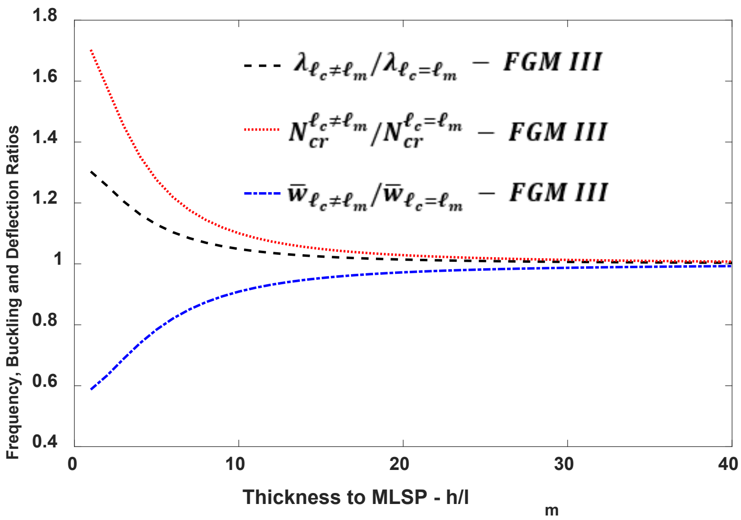

c) FGM III

Figure 3. Ratio of DFFs, DCBLs and DMDs of S-S FG porous microbeams between the results of MSGT obtained from variable MLPS ($\ell_m \neq \ell_c \neq \ell$) and constant MLSP ($\ell_m = \ell_c \neq \ell$) with respect to (h/ℓ_m) $(L/h = 10, p_z = 1, \alpha_0 = 0.1)$

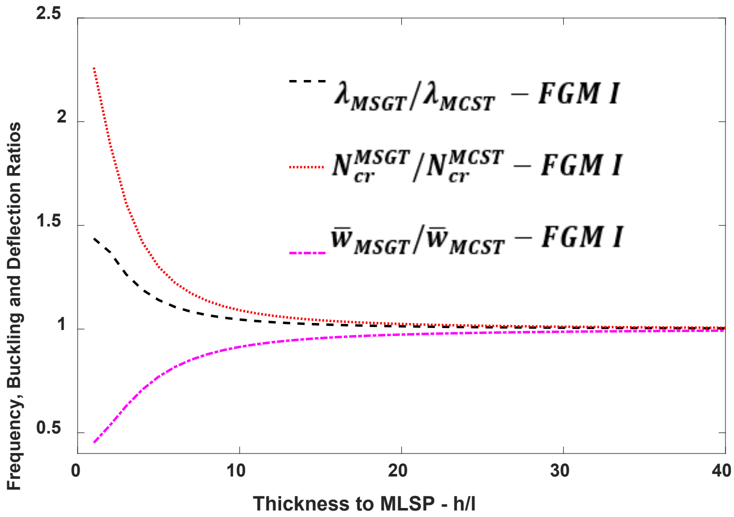

a) FGM I

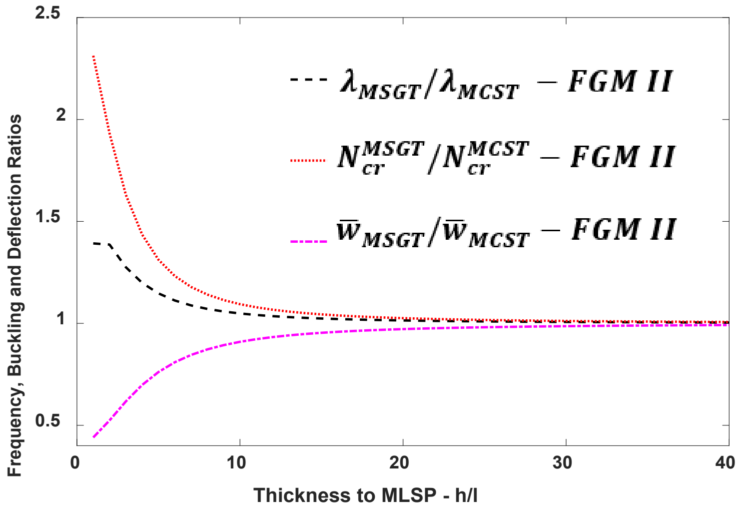

b) FGM II

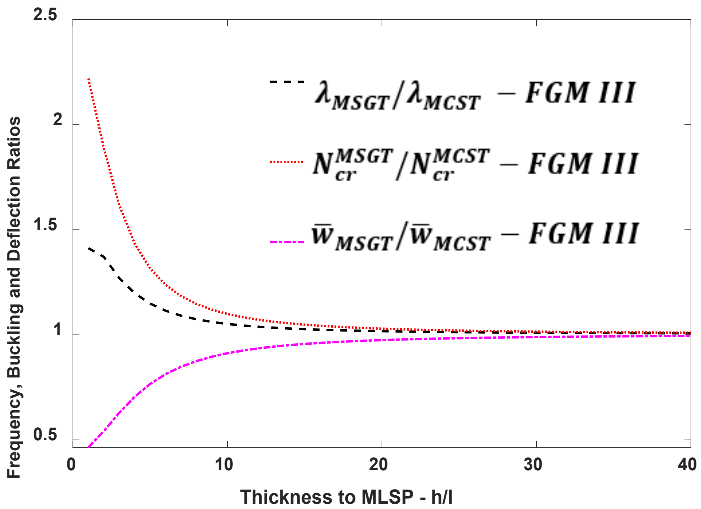

c) FGM III

Figure 4. Ratio of DFFs, DCBLs and DMDs between MSGT and MCST for C-C FG porous microbeams with respect to (h/ℓ_m) $(L/h = 5, p_z = 1, \alpha_0 = 0.1, \ell_m = \ell_c \neq \ell)$

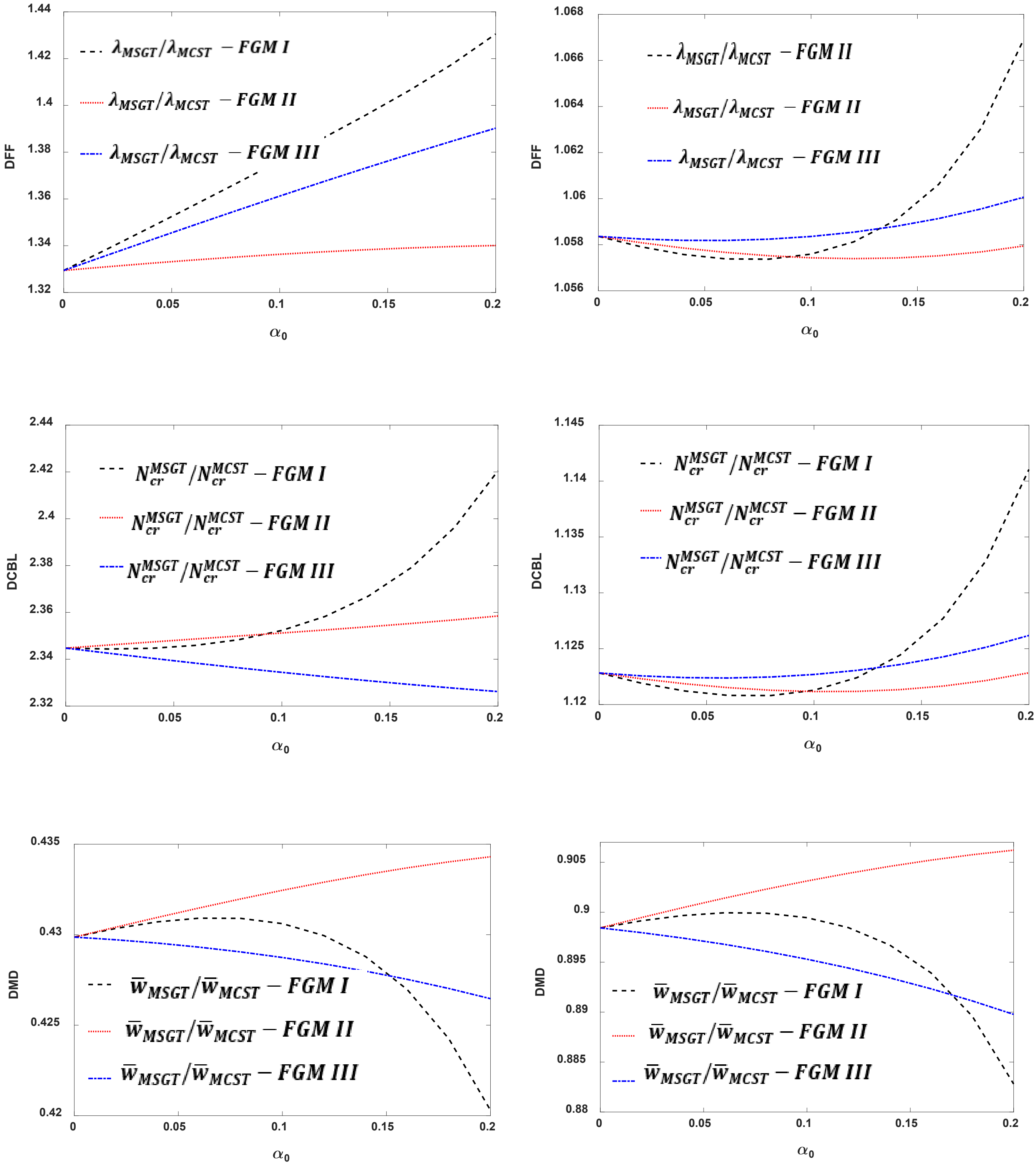

$h/\ell_m = 1$ $\qquad$ $h/\ell_m = 8$

Figure 5. Ratio of DFFs, DCBLs and DMDs between MSGT and MCST for S-S FG porous microbeams with respect to α_0 $(L/h = 5, p_z = 5, h/\ell_m = 1, 8, \ell_m = \ell_c \neq \ell)$

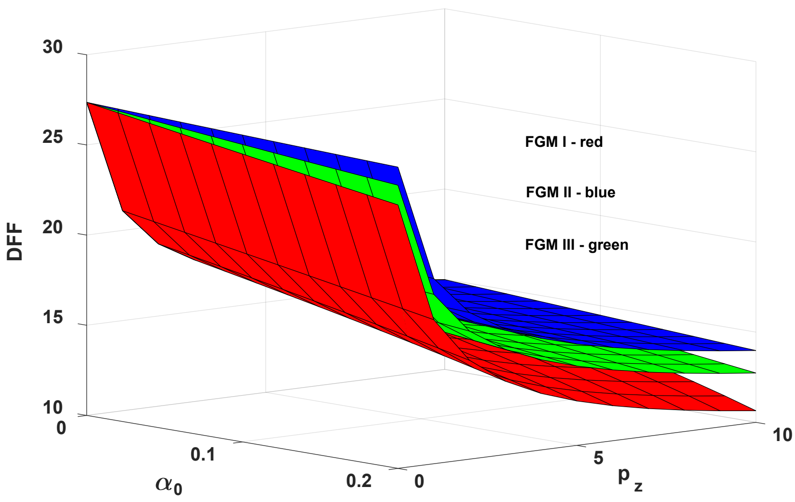

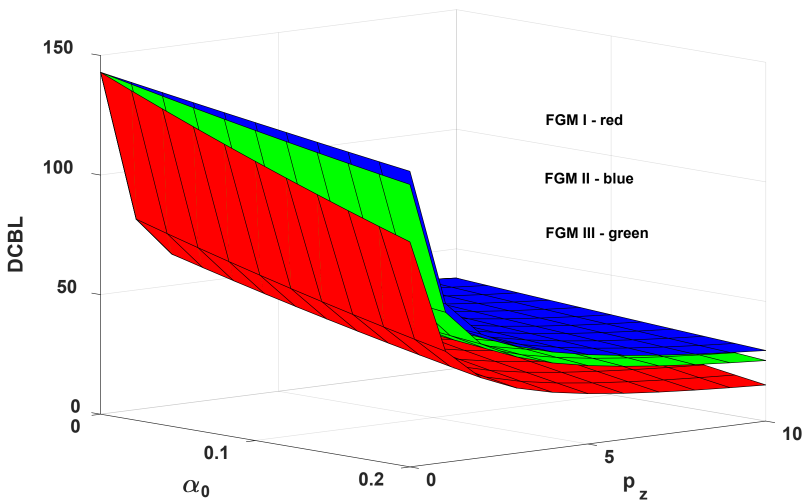

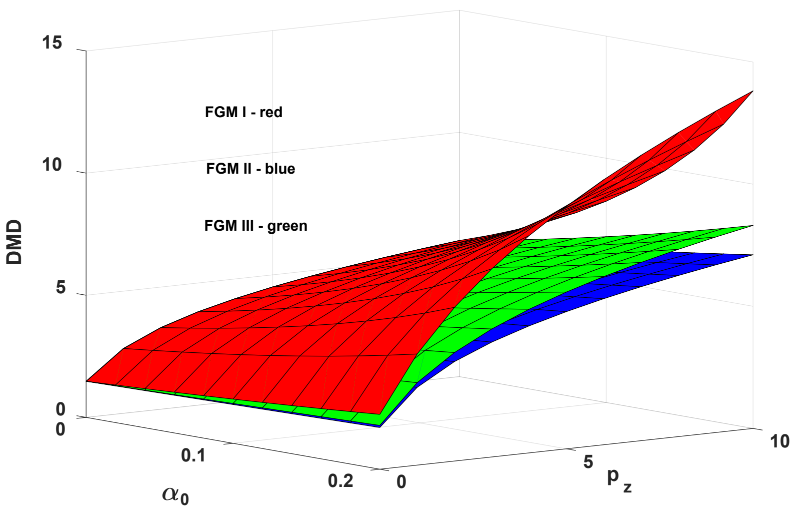

Figure 6. DFFs, DCBLs and DMDs of C-C FG porous microbeams with respect to α_0 and p_z $(h/\ell_m = 2, L/h = 5, \ell_m = \ell_c \neq \ell)$

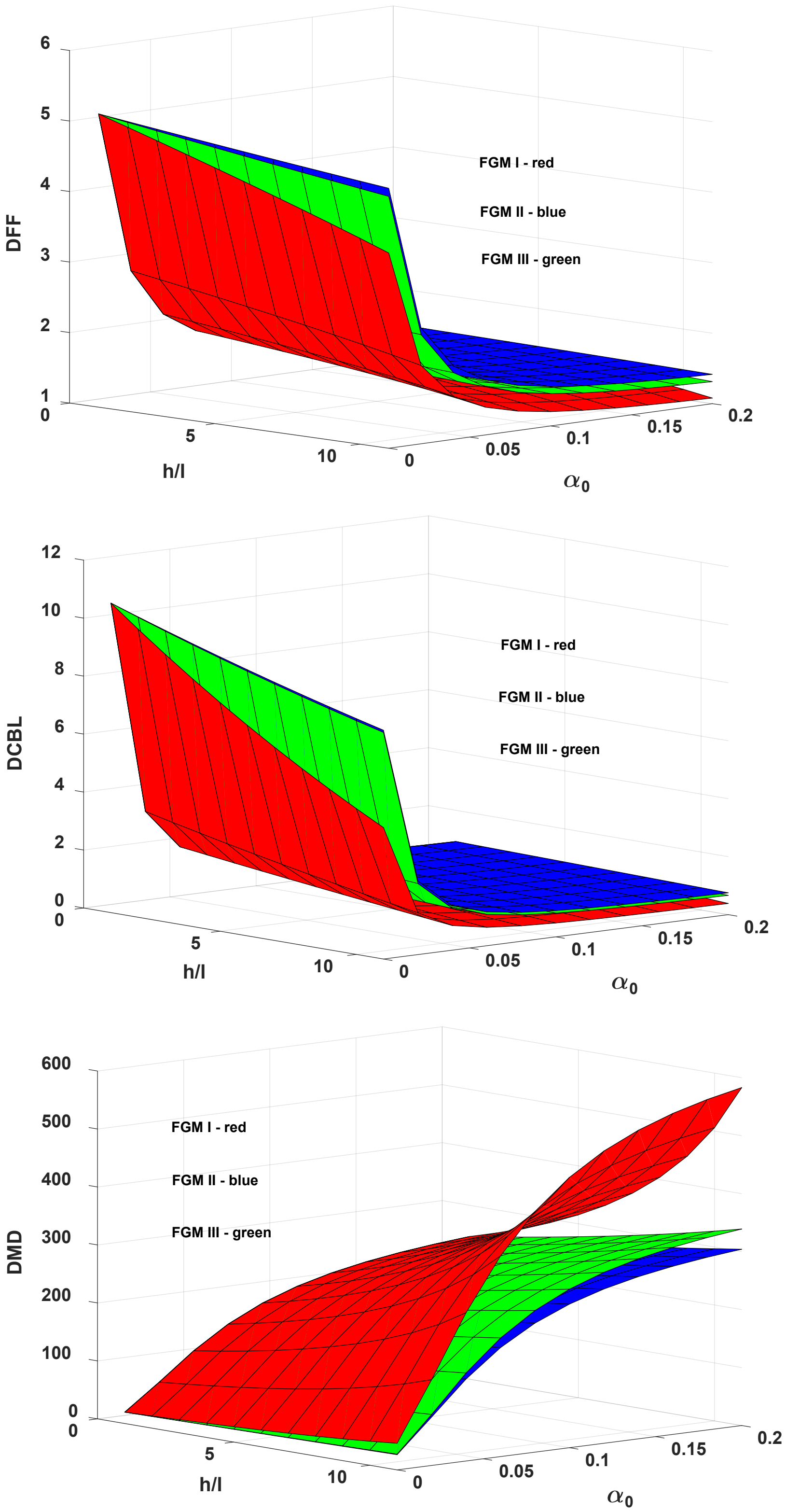

Figure 7. DFFs, DCBLs and DMDs of C–F FG porous microbeams with respect to α_0 and (h/ℓ_m) $(p_z = 5, L/h = 5, \ell_m = \ell_c \neq \ell)$

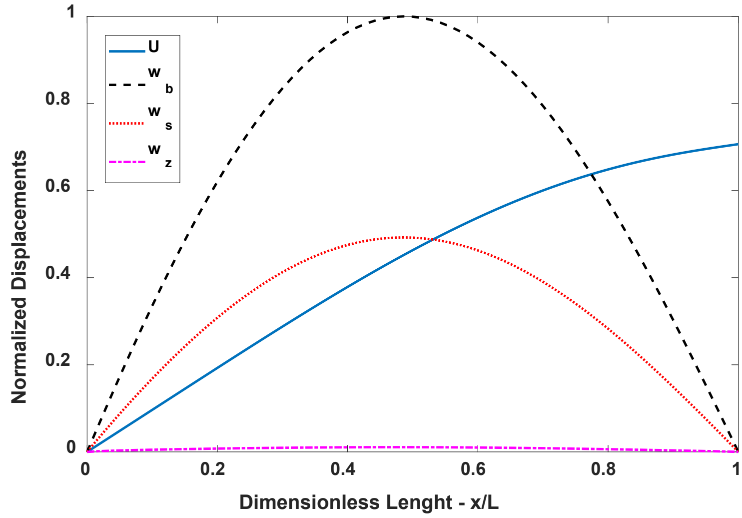

a) FGM I

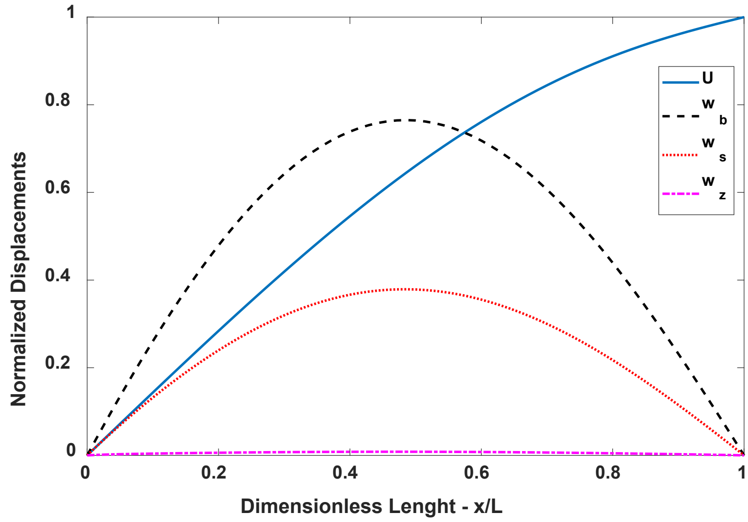

b) FGM II

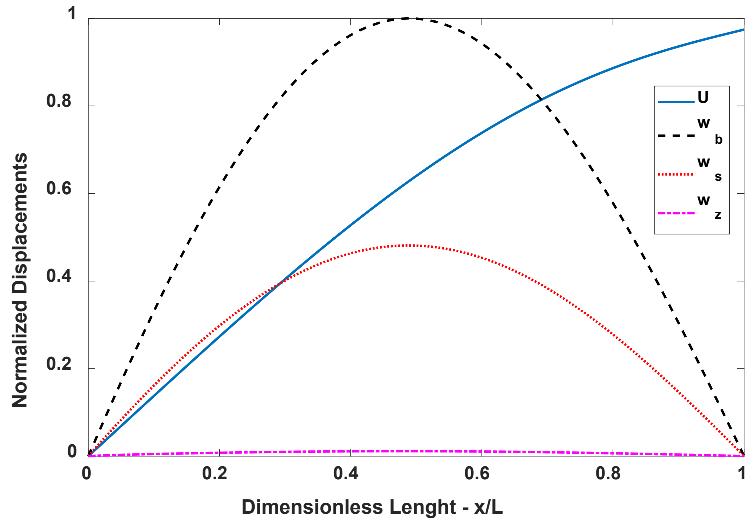

c) FGM III

Figure 8. The first vibration mode shapes of S-S FG porous microbeams ($\alpha_0 = 0.2, h/\ell_m = 1, p_z = 5, L/h = 5, \ell_m = \ell_c \neq \ell$)